Chapter 16
Prevent Leakage and Mixture of Karst Groundwater

Saša Milanović, Veselin Dragišić, Milan M. Radulović and Zoran Stevanović

16.1 Choosing Optimal Dam Sites and Preventing Leakage from Reservoirs

Saša Milanović

Centre for Karst Hydrogeology, Department of Hydrogeology, Faculty of Mining and Geology, University of Belgrade, Belgrade, Serbia

16.1.1 Introduction

With respect to risk factors in the dam and the reservoir construction in karst, particular attention must be paid to choosing optimal dam sites and preventing leakage from reservoirs (Milanović et al. 2010). An appropriate project concept prior to exploration can significantly reduce the risks of water losses or at least minimize them to

S. Milanović (✉) · Z. Stevanović
Centre for Karst Hydrogeology, Department of Hydrogeology,
Faculty of Mining and Geology, University of Belgrade, Belgrade, Serbia
e-mail: sasa.milanovic@rgf.bg.ac.rs

Z. Stevanović
e-mail: zstev_2000@yahoo.co.uk

V. Dragišić
Department of Hydrogeology, Faculty of Mining and Geology,
University of Belgrade, Belgrade, Serbia
e-mail: v.dragisic@rgf.bg.ac.rs

M.M. Radulović
Faculty of Civil Engineering, University of Montenegro,
Cetinjski put bb, 81000 Podgorica, Montenegro
e-mail: radulovicmilan33@yahoo.com

Z. Stevanović (ed.), *Karst Aquifers – Characterization and Engineering*,
Professional Practice in Earth Sciences, DOI 10.1007/978-3-319-12850-4_16

acceptable levels (Therond 1972; Zogović 1980; Milanović 2000a; Bruce 2003; Ford and Williams 2007a; Fazeli 2007), while the absence or reduction of exploratory works can increase them (Sahuquillo 1985). Milanović et al. (2010) stated that many analyses show that once the reservoir is filled up, groundwater flow often reactivates currently unsaturated (fossilized conduits) pathways and form a reverse discharge outside of the reservoir area. In response to these findings, it is of great importance that at an early stage of the research, the main emphasis must be on the establishing of the complex conditions of karst groundwater circulation genesis. As discussed in Chap. 13, some inadequately explored dam sites or reservoirs constructed in karst have never fully filled up with water or have been abandoned after unsuccessful attempts to reduce enormous water losses. Others have had sudden water losses even after years of successful operation or increases during years of operation. However, construction of the dam and reservoir in karst does not automatically result in a leakage problem by choosing optimal dam sites with suitable geological and hydrogeological conditions, leakage problems can be partially or totally avoided (Milanović 2000a).

16.1.2 General Overview of Procedures for Preventing Leakage and Choosing Dam Sites

Choosing optimal dam sites is a very complicated task due to the nature of karst and the insecurity of water storage due to leakage from reservoirs. In this regard, a few preliminary questions of great importance must be raised and answered:

1. How do we select an appropriate location for the dam and reservoir?
2. How do we select appropriate investigation methods?
3. What are the main tasks during investigations?
4. Is our survey sufficient to provide answers about the general feasibility of the project?
5. Will the data expected from the survey be sufficient for a proper assessment of potential water losses?
6. Can we find a technical solution either to avoid leakage or reduce it to an acceptable level?

The answers to the last three of these six questions depend strongly on positive answers to the first three questions. And even though a guarantee of reservoir or grout curtain tightness is unlikely, the risk of large water losses can be minimized (Milanovic 2000). Based on previous approaches to leakage from reservoirs applied, the proposed methodology should be applied in the most probable leakage zones and pathways at the dam site and reservoir and can be highlighted generally as three cases:

- dam sites and reservoirs in karst poljes—leakage in different directions through Quaternary deposits on the bottom of polje (probability of high risk),
- dam sites and reservoirs in river valleys—leakage usually below the dam site, in the direction of the river stream (medium to high risk),
- dam sites in deep and narrow canyons with different morphology than in the reservoir area—leakage through dam site banks (medium risk).

Fig. 16.1 Reinforced concrete cylindrical dam around Opačica ponor (sinkhole) (*left*); non-returned valve constructed on some small sinkhole in the area of Vrtac Reservoir in Nikšić polje (*right*)

A variety of dam sites may be suitable for potential dam construction, but investigation of the relevant geological and hydrogeological factors and issues will reveal which sites will best achieve the aim of water tightness, while still fulfilling the intended purpose of the proposed dam and reservoir.

From the hydrogeological point of view, karst poljes are probably the most complex areas for dam and reservoir construction. Usually, wide and very large zones of concentrated infiltration and discharge are located in these depressions. And usually, when the bottom of the polje consists of impervious strata, some sinkholes, estavelles, and intermittent springs are situated along the foothills. If alluvial deposits cover the bottom, the zones of concentrated infiltration can occur everywhere. As previously indicated, one good example is the reservoir at Vrtac with its enormous losses (27 m^3/s) (Vlahović 2005). However, after considerable work performed on the sinking zones by constructing cylindrical dams (Fig. 16.1) and non-returned valves, losses are not reduced at all.

A dam site can be located in narrow karstic canyons where the riverbeds are usually the deepest erosion base levels. In this case, the karstic features (different kinds of conduits) below the river bottom are usually very rare and only in some cases can be predisposed by hypogene karstification. In such cases, the water table is either connected with or very close to the riverbed, and dam sites are generally reasonably impermeable. Still, the dam site and reservoir banks can be prone to leakage. Solving the problem of the water tightness of banks can sometimes be very complicated. Salman Farsi dam in Iran is a good example of finding karstification as a main water tightness problem on dam site banks and both abutments (Box 16.1.1).

Very often, the spatial position of dam sites and reservoirs is located in karstic river valleys. Choosing optimal dam sites as well as preventing leakage from reservoirs, there needs more attention than in the case of canyon sites. Usually, the base of karstification is below the riverbed, and the presence of huge karst conduits (caverns and channels) can be hundreds of meters below the river or future reservoir bottom (Box 16.1.2). Reactivation of old deep conduits due to huge pressures from reservoir water is often a problem in these cases.

During the dry period of the year, the groundwater level is deep below the surface, while during the high water period, the water table rises abruptly and a considerable part of the bottom is under the influence of a strong uplift. The most common and unpredictable defects found during reservoir operation are karst channels naturally plugged by clay and covered by alluvium and *terra rossa* and reactivated by water pressure, suffusion, or air pressure effect (Milanović 2000a). As a result, collapses, holes, and huge open cracks in the reservoir bottom appear. Many examples of dams and reservoirs (successful constructions or total failures in terms of water tightness) in karst poljes illustrate the complexity of karst hydrogeology in dam and reservoir constructions.

Generally, the investigations should be very serious and decisions on water tightness treatment (during construction or later remediation work during exploitation) should be carefully provided and analyzed. Those investigations are focused on the one hand on defining the type of underground and deep treatment, and on the other hand, on surface treatment (Box 16.1.3).

The provision of good quality geological and hydrogeological data is necessary to establish a crucial base for making correct decisions in the process of choosing optimal dam sites and preventing leakage from reservoirs. Also, the geological, hydrogeological, speleological, and other special investigation procedures should be a permanent activity during the design stage, during the construction of the dam site and filling of the reservoir, as well as during exploitation. Having a good map, database, models, and geological, hydrogeological, and other 2D and 3D layers increases the chances of successful dam site choosing and minimizes the possibilities of further leakage from reservoirs below the dam site and through the reservoir and dam site bankment. The following procedure is necessary for the acquisition of some of the basic information (with characteristic examples) for choosing an optimal dam site and preventing leakage from reservoirs in karst formations:

1. Detailed surface geomorphological analysis of reservoir and dam site area,
2. Speleological and cave diving as analysis of karst interior,
3. Detailed hydrogeological analysis of characteristics of lithological units,
4. Structural analysis of the spatial position of folded structures, especially the hydrogeological role of anticline core,
5. Analysis of characteristics of main faults (elongation, depth, nature of crushing material between tectonic blocks, and disturbance of ruptures by karstification),
6. Analysis of tracer tests data as a base for groundwater flow defining,
7. Detailed analysis of speleogenesis,
8. Detailed analysis of karst conduit distribution,
9. Analysis of groundwater monitoring data of the wider area (fluctuation, defining minimum, and maximum level of water table, etc.),
10. Detailed analysis of the investigation borehole (thermal methods, borehole radar, different geophysical logging methods, core analysis, TV logging of borehole, etc.),

11. Excavation of investigation and grouting galleries and its arrangement are very important. All huge open caverns should be directly observed using access galleries and shafts. The vertical distance between grouting galleries should be less than 50 m (Milanović 2000a),
12. Analysis of water pressure tests,
13. Forming 3D spatial and physical models of the reservoir and dam site area.

Box 16.1.1

Case Study—Salman Farsi dam—Preventing possible leaking problem during construction

Salman Farsi Dam (125 m high) is located on the Ghareh-Agaj River in Fars province, in southern Iran (Fig. 16.2). From the geological and hydrogeological point of view, this dam is one of the most complicated sites in Iran.

Fig. 16.2 Photo of dam site during construction and Salman Farsi Dam in the last stage of building

During the excavation of grouting galleries, some large caves at both abutments were discovered (see Sect. 15.4, Box 15.4.5). The volume of the biggest one (Golshan's Cave) exceeds 150,000 m^3. Due to these conditions, large-scale underground geotechnical treatment was needed to prevent leaking and improve the water tightness of the dam site. The main question was how to prevent leaking through the dam abutments (Fig. 16.3).

The dam site is located in the northern flank of the Changal anticline, whose hydrogeological characteristics played a key role in the choice of the dam site. The Pabdeh Formation downstream of the dam site (consisting of marl and shale layers) is located in the core of the anticline. This formation has acted like a thick and deep impervious barrier against underground water filtration from the upper erosion base levels to the lower levels (Fig. 16.3), which is also the key function of the water tightness of the Salman Farsi grout curtain heading downstream. However, upon finding large caverns in the abutments of the dam site, the question of water tightness and how to prevent leaking from the reservoir. DEM with main faults and the spatial position of the dam, grouting gallery, and Golshan's Cave are shown on Fig. 16.4.

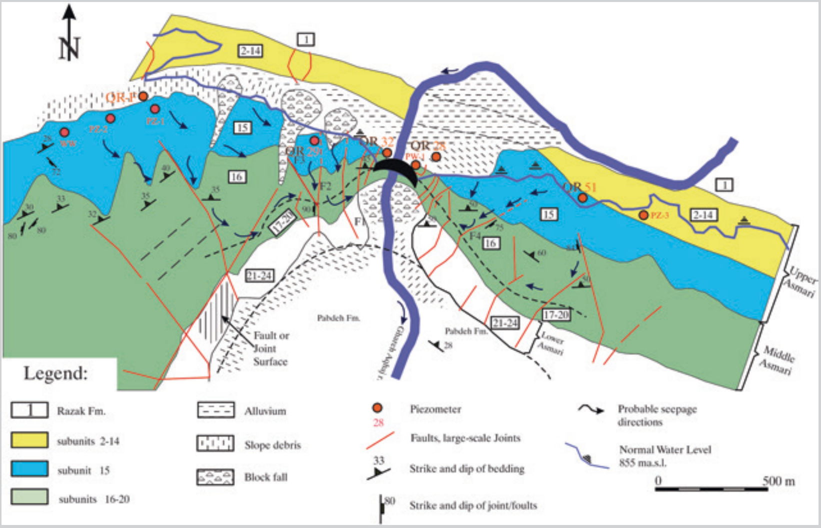

Fig. 16.3 Geological sketch of dam area (Fazeli 2005)

During the folding process, the anticline is disturbed by some fractures, faults, and joint sets. Some of them are distinguished at the dam site. From the point of view of water tightness, two of them are very important: faults with the strike of NE–SW and other sets of faults with the strike of N–S (Fig. 16.3). Both sets are subvertical (dip about 80°). The dip of the bedding planes is 50–60 degrees toward upstream (Fazeli 2005). Well-developed faults sets together with steep joints and bedding planes have made a well-connected network for water filtration.

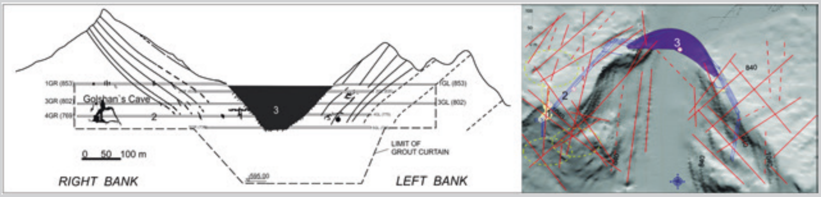

Fig. 16.4 DEM of dam site with spatial position of the main caverns, grouting galleries, and faults. *1* Golshan’s Cave, *2* Grouting galleries, and *3* Salman Farsi Dam

Prevent leaking through dam abutments—grouting gallery redesign

The construction of a grout curtain in dam abutments with a highly random distribution of caverns and channels has some uncertainties. After the discovery of caverns during the excavation of grouting galleries (see Sect. 15.4, Box 15.4.5), it was necessary to make some redesigns in order to prevent leakage of water from the reservoir.

Cleaning of the caverns and caves entails removing all kinds of material (clay deposits, blocks, crushed material, and water) from the investigated caverns and caves. Usually, removal of the materials and cleaning will continue until sound rock is reached. It often needs some extra shaft and gallery excavation as well as blasting. Cavern treatment was provided 20 m upstream and 10 m downstream of the curtain. In the Salman Farsi Dam, it took years to clean some big caverns (Fig. 16.5).

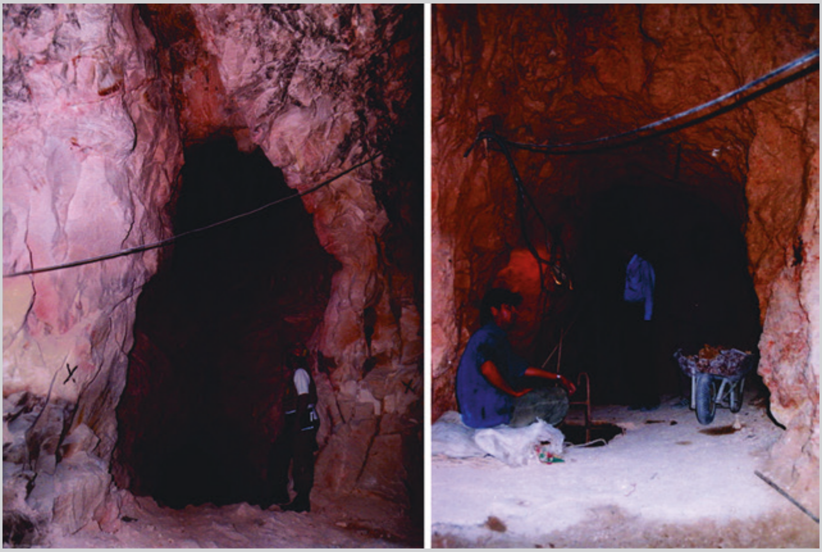

Fig. 16.5 *Left*—geological investigation in grouting galleries, *Right*—cleaning of the caverns

Then after, the following measures were also applied:

1. All caverns and caves which are accessible and do not have a big volume were filled with concrete. Also, caverns with a big volume, and where the spatial position is only a few meters upstream and downstream of the curtain, were filled (this is called concrete plug).
2. Final grouting is performed after executing the concrete plug. This grouting is done to fill the empty spaces between the concrete and rock by grouting.
3. After completing the above phases, drilling new grouting holes and connecting the curtain to the plug are recommended.

In response to new data, it was decided that an upstream bypass of Golshan's cave is the best solution. Four galleries (853R, 802R, 769R, and 738R) were shifted upstream of Golshan's cave, and the grout curtain was extended by 1,560 m (Fig. 16.6). The karst treatment took about 1.5 year, but the final results seem satisfactory. The karst treatment was done and it took only 1,020 m^3 to fill the karst with concrete. The old route of the curtain will be used to monitor the curtain performance.

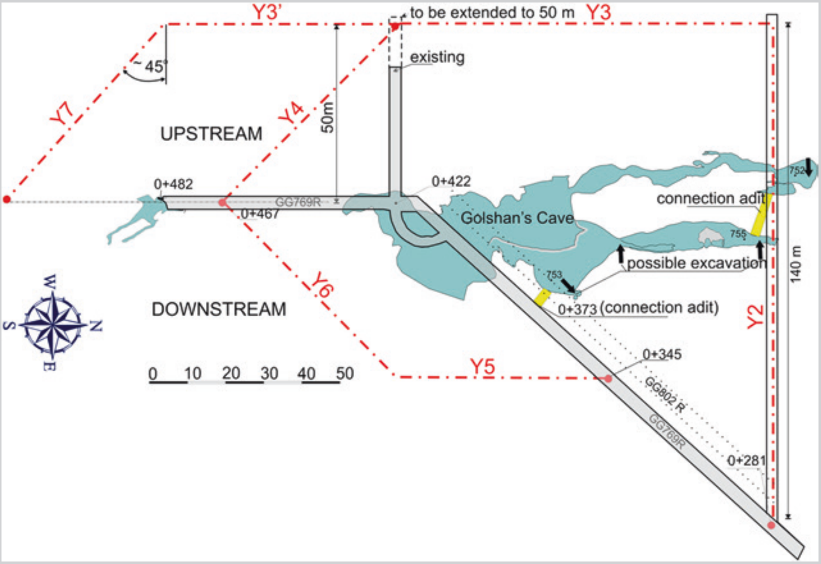

Fig. 16.6 Grout curtain bypass (Layout of Golshan's Cave after D. Vučković, S. Milanović, 2001, Salman Farsi (Ghir) Dam Project, Speleological Investigations, Mission Report), unpublished, (From Stucky-Electrowatt 1996–2004 and Fazeli 2005)

Box 16.1.2

Case example—Problem of karstification (leakage) below the Ourkiss dam site

The Ourkiss dam site is located 5 km from the city Oum el Bouaghi (NE Algeria) at the entrance of Oued Ourkiss gorge. Oued Ourkiss is one of the tributaries of the salty lake Garaet el Guelif. The wide valley inside the future reservoir consists of Miopliocene and Quaternary deposits which overlie the Albian and Aptian well—karstified limestones. A rock-filled dam with clay core is proposed in the gorge cutting the limestone outcrops (Fig. 16.7).

Fig. 16.7 Ourkiss dam site and reservoir area during construction

The designed reservoir at the altitude of 951 m a.s.l. will store the waters of the temporary Oued Ourkiss stream, but over 90 % will flow in as waters pumped from another reservoir, the Oued Athmenia (Stevanović et al. 2010). The dam height is 35 m with a crest length of 400 m, width of 8 m, and width of foundation of 216 m.

This case example summarizes the analysis of important discontinuity systems and their role in karst genesis at the dam site. The Ourkiss dam site was developed in limestone rock, under particular hydraulic and structural conditions. Therefore, these karst systems are composed of many segments (small channels, caverns with speleo forms, shafts, cracks, etc.), each of which is contained entirely by distinct discontinuities, such as bedding planes, joints and fractures, faults, or along interception of those structures. Survey of those structural elements is the initial step in definition of pathways of the groundwater circulation. The most important task for the future prevention of leakage below the dam site, however, is to know exactly what the karst process and level of karstification (depth and spatial position) are.

Results and discussion

The geological setting indicated possible water losses from a new reservoir. Moreover, during one of the floods, a large amount of water sunk into one of the discovered ponors. After an almost complete loss of large amounts of water, excavation was carried out at the dam site and its right side is a registered cavern with a length of 0.5 m (240/60), and which can be visually traced to approximately 20 m deep. Following the discovery of the caverns, further research in the area of the dam has devoted far more attention to possible indicators of intense karstification. Performed by gravimetric measurements on a wider profile dam, a strong anomaly at the dam site was also noted. In order to collect sufficient data for possible protective measures such as grouting and impermeable blanket, (Milanović et al. 2007) an investigation program has been defined.

Generally, some methods can, however, help to lessen the probability of undesired effects. Direct observation of interior karst was the first among different methods applied at the Ourkiss dam site. Recording of karstified pathways by a specially constructed video camera was more effective in this case than some geophysical methods as well as, logging, caliper or tracing (Fig. 16.8). Recording of open caverns and boreholes on both embankments of the Ourkiss Dam very much helped to orient further exploration and to define protective measures which include sealing and the construction of an impermeable clay blanket in the wider area (S. Milanović, 2007, Results of recording of karstic features—Ourkiss dam project. Report. Hidrotehnika, Belgrade, 2012).

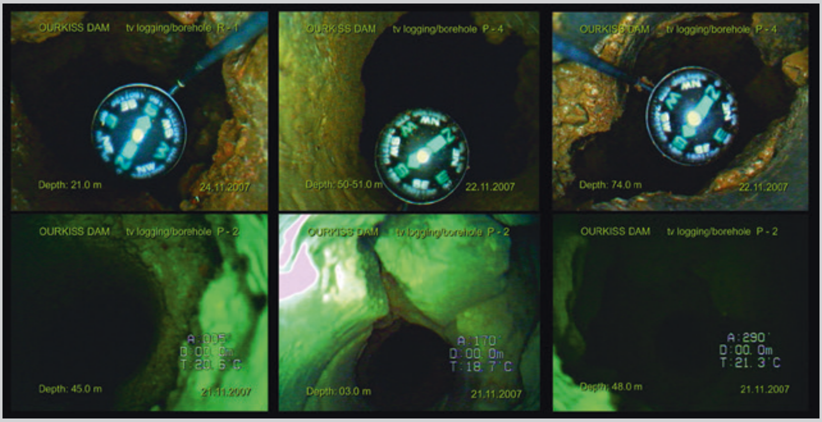

Fig. 16.8 Some of the recorded caverns in the boreholes at the Ourkiss dam site

The inventory covers a large number of cavities, in total 460 in ten surveyed boreholes (Table 16.1). Most of those cavities are currently above maximal groundwater table, but will be fully impounded after the reservoir filling.

Table 16.1 The results of camera recording of karst conduit network at the Ourkiss dam site

Borehole	Elevation (m a.s.l.)	Depth (m)	GWL (m a.s.l.)	No. of karstified intervals	General direction/^{0}	Maximum length (m)	Minimum length (m)	Calculated porosity (%)
P2	919.57	62		28	325–335	9	0.1	12.1
P3	923.62	67	863.62	19	335–360	4	0.3	7.3
P4	939.13	85	854.13	22	300–325	5	0.2	8.2
R1	924.5	74		16	295–318	4	0.25	4.1
R2	913.75	50	863.75	14	310–322	3	0.1	1.9
R3	932.35	60		19	288–303	3	0.1	2.2
R4	932.65	78	857.65	17	310–340	2	0.05	1.5
GD-III-25	921.25	33		9	312–345	3	0.2	1.7
GD-III-30	921.08	37.5		4	300–330	2	0.3	1.8
GD-III-35	920.97	42		5	290–325	3	0.25	2.1

Based on this survey, the sealing of the main shafts and the construction of an impermeable blanket in the wider area are proposed.

The spatially large and deep Ourkiss conduit system would probably not be fully explored by using conventional geophysical or other remote methods for the following reasons:

- The caliper's bars are too short to record the size of the found cavities.
- Tracing tests provide valuable information through recorded velocities or tracer quantitative analyses, but cannot be successfully conducted in unsaturated parts.
- Good information about the size and volume of empty space can be obtained by a water injection test into wells, but there are also many obstacles. For example, a large amount of water can be absorbed even by a small, but well-connected fissure system. This means that water losses registered by the classical test do not provide sufficient data to distinguish enormous from medium-sized or even small cavities.

Lastly, obtained photos or movies recorded by camera are also, at most, relative proof. Although powerful, the lamp can still be insufficient to light the furthest or curved parts. Besides, similar to the above-mentioned methods, the camera evidence will not result in absolute values of storativity, but will always provide better insight into situations and orient further research (Fig. 16.9).

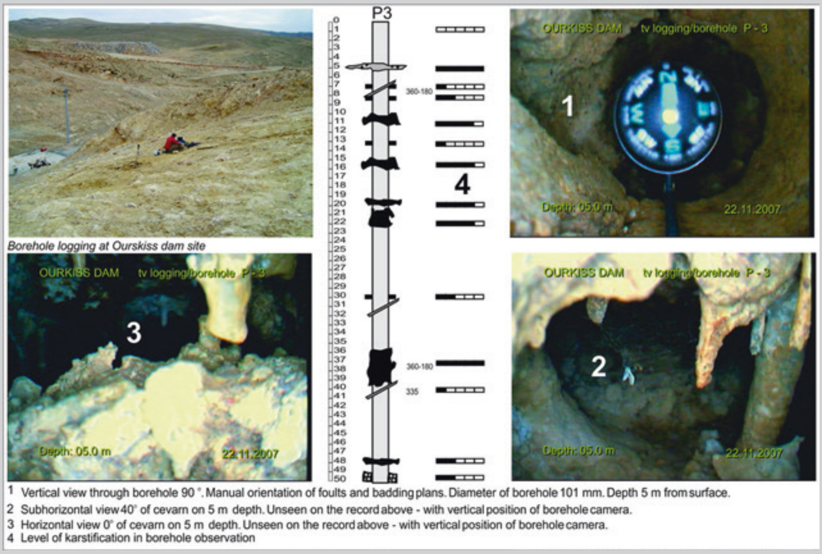

Fig. 16.9 Detail of borehole P-3 video logging

Data of monitoring boreholes with detailed zones of karstification are shown on the comparative cross sections on Fig. 16.10

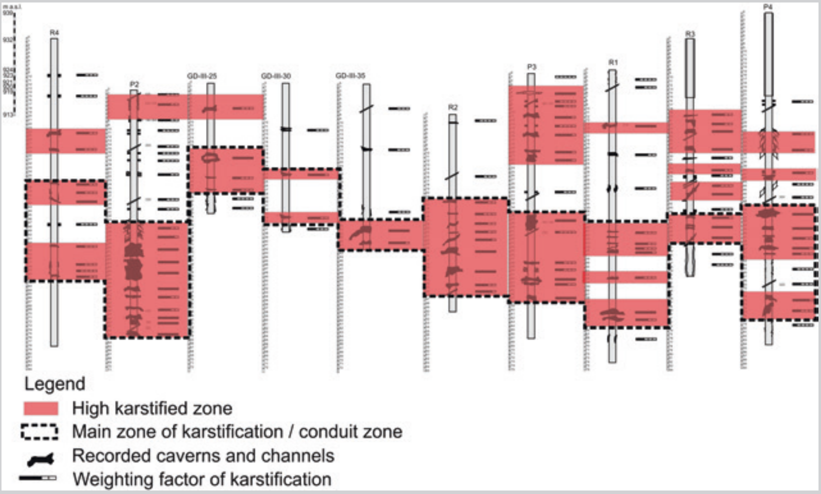

Fig. 16.10 Cross section of boreholes with data of karstified zones

In all boreholes, in parallel with the drilling, experiments concerning test permeability were carried out (Lugeon test). The greatest losses of over 100 Lu were registered in the borehole on the left bank P-4 (45–50 m) and downstream in the river valley, in P2 (45–50, 60–65, and 65–70 m).

For purposes of correlation, data of karstification in the narrow zone of the dam site at Ourkiss, and a detailed layout and cross section of all known karst forms of the borehole were made, as shown on Fig. 16.10. The borehole video logging data and borehole profiles previously derived from zones of karstification in Table 16.1 show the spatial development of the main karstified zone at the dam site at Ourkiss (Fig. 16.11).

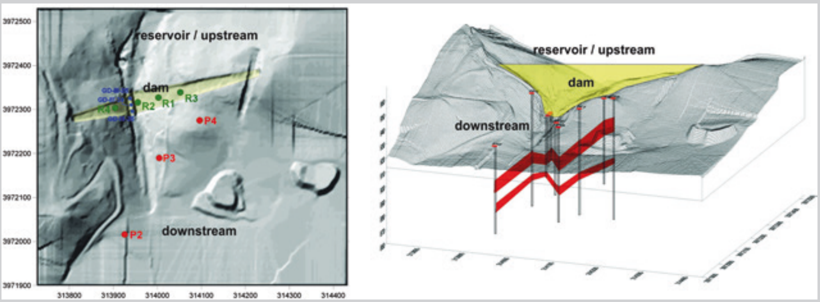

Fig. 16.11 DEM of Ourkiss dam site with investigation borehole position (*left*); 3D model of main karstification distribution (*right*)

On the basis of data obtained during research in the area of the dam site and reservoir area as a solution for the Ourkiss project leakage under the dam body, three solutions were considered.

1. underground sealing—grout curtain,
2. surface sealing (impermeable carpet)—geomembrane and geotextile, and
3. surface sealing—shotcrete.

Upon analysis of all the alternative solutions, it was concluded that the second solution and the use of geomembrane and geotextile will be the most trusted solution for this condition for highly developed karstification and very insecure and troubled grouting. Finally, for preventing leakage under the dam site as well as in the reservoir area, an impermeable carpet was made geomembrane (520,000 m^2) and geotextile (550,000 m^2) (Fig. 16.12).

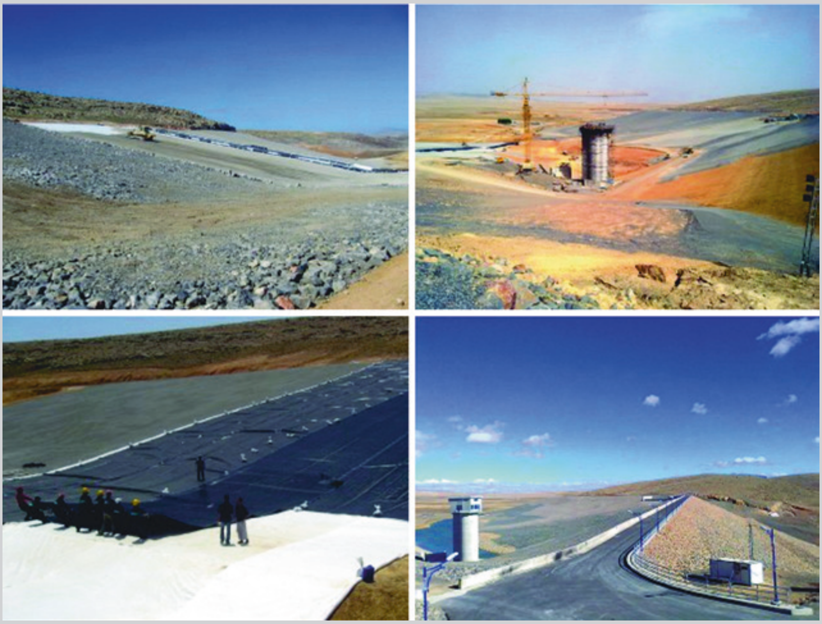

Fig. 16.12 Photos from the phase of impermeable carpet installation (geomembrane and geotextile) http://www.hidrotehnika.rs/alzir/brana-ourkiss/

Box 16.1.3

Case Study—Višegrad dam—Problem of increasing leakage during exploitation (current investigation)

The Višegrad hydropower plant is situated in Dinaric karst on the River Drina, 2.7 km upstream from the town of Višegrad (Bosnia and Herzegovina). It was built from 1985 to 1989. The dam of the Višegrad HPP is a concrete gravity dam. An integral part of the dam is the 594-m-long grouting curtain (325 m beneath the dam structure and 65 m in the left abutment and 204 m in the right abutment) and 50–130 m deep. Investigation works related to the development of the dam and power plant began in 1976, and the design documentation for the principal objects that constitute the power plant was developed before 1983.

Already in the first year of the exploitation of the Višegrad dam, the occurrence of submerged downstream springs was noticed. From the measurements of water quantities that appear in the springs downstream from the dam, it was established that the quantity had increased from the 1.4 m^3/s (in 1990) to 13.92 m^3/s (in 2008), and 14.68–15.00 m^3/s (in the 2012) (Fig. 16.13). In order to define the positions of karst conduits along which the groundwater circulates under the dam site, in 2009 and again in 2013, special-purpose investigations and remediation works (still in progress) were performed. Geological investigations of the karst setting, required to address leakage beneath the Višegrad dam, were focused on a rather narrow area containing a refill "sinking" zone and a drainage "discharge" zone. The basic problem was how to perform a quality analysis, or how to state the problem whose goal was to reduce or to stop leakage below the dam site. The problem was approached from three parallel directions: a theoretical approach, which initially played a major role and provided guidelines for field activities; detailed and highly complex field investigations and development of a basic input 3D model; and an empirical approach and later also a mathematical approach aimed at producing the final form of the model.

Fig. 16.13 *Left*—Submerged discharge points during tracer test (*downstream*, *left photo*); Spatial position of main sinkhole (location of tracer injection at a depth of 50 m) (*upstream/reservoir*; *right photo*)

Overview of results during previous investigations, design construction, and exploitation

Geological investigations were performed during all phases of design and construction of the dam of the Višegrad HPP. During the previous period of dam exploitation, certain multidisciplinary investigations were also performed, primarily with the goal of choosing the optimum dam site as well as definition of possible seepage. All these investigations have yielded a large body of results, a part of which is significant for the solution of the leakage problem under present conditions below the dam site.

For the needs of the development of the main project, within the scope of the development of geological data relevant to dam construction, detailed geological mapping of the dam site (in the 1:50–1:1000 scale) had been performed. Mapping of the catchment area of the Višegrad reservoir and dam site was performed on the scale of 1:10000, while an engineering geological map of the dam site was performed on the scale of 1:500. Engineering geological mapping of the foundation tectonic was performed during the course of excavation of the dam foundation and riverbed downstream. Some of the investigative drilling was completed during the course of the development of the preliminary design, but most of it was performed during the preparation of the basic design. More than 4,470 m of drilling was performed during previous investigation phases together with water pressure tests WPTs. Also, groundwater tracer tests were performed in the phase of choosing the optimal dam site. Systematic monitoring from the stage of previous investigation and design construction up to the exploitation of water seepage beneath the dam has been done from 1991 to the present (Fig. 16.14) (Institute for Development of Water Resources "Jaroslav Černi", 2009, Design on rehabilitation regarding water seepage beneath the dam of the Višegrad hydropower plant, Summary Report on Performed Investigations, Belgrade, unpublished).

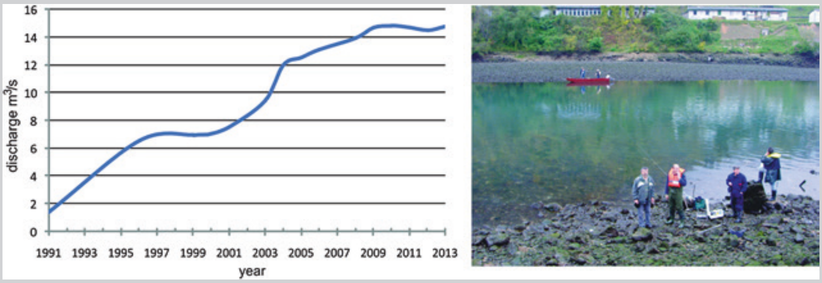

Fig. 16.14 Diagram of water discharge (seepage) through time (*left*). Measuring discharge from springs (*right*)

Groundwater levels were also monitored in the piezometers located in dam abutments and abutment injection galleries during the course of trial filling and then on a continuous basis through the years 1991, 1994, and 1995. At present, the groundwater level regime is monitored twice a month in 58 piezometers.

Outline of results of special-purpose investigations

In 2009, special-purpose investigations were performed in order to define the conduits along which the water leakage occurs below the dam site. Since the study and systematization of the results of previous investigations generally shown above, the investigations have started with the determination of the geological structure of the wider area of the Višegrad reservoir that encompassed an area of cca. 6 km^2. The first step was remote sensing investigations, based on the analysis of satellite images and aerophoto images from the period before the construction of the reservoir. Along with that, the geological mapping of the terrain was performed, with the corresponding petrologic investigations and detailed ruptural investigations. Detailed investigations of the narrower area around the dam site started with the geodetical survey of the dam and the appurtenant structures on the scale of 1:1000 (Institute for Development of Water Resources "Jaroslav Černi", 2009, Design on rehabilitation regarding water seepage beneath the dam of the Višegrad hydropower plant, Summary Report on Performed Investigations, Belgrade, unpublished). Geological investigations of the dam site started with new, high-quality detailed geological mapping of the terrain (Fig. 16.15). Parallel with these investigations, cross-hole geoelectric scanning in the left and right dam abutment and over the reservoir was performed, as well as reflective seismic investigations in dam galleries.

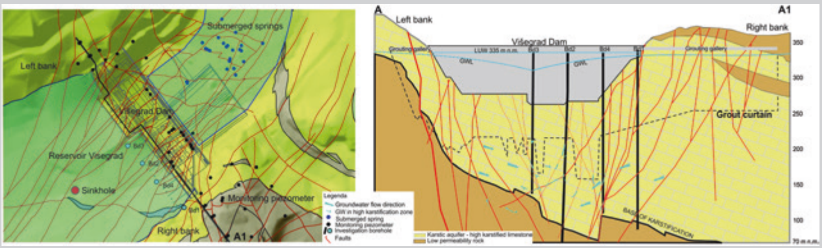

Fig. 16.15 Hydrogeological map and cross section of Višegrad dam site with position of grout curtain and investigation boreholes

The bathymetric recording of the bottom of the part of the storage near the dam and measurement of self-potential were performed simultaneously in the storage zone. These investigations in the storage zone led to the detection of anomalous locations that indicated possible water percolation. At locations of detected anomalies, detailed diving investigations and underwater video camera recordings were also performed. These investigations revealed the existence of a sinkhole of great size and capacity, which had an impact on the adjustment and re-direction of the subsequent investigations. Immediately after the detection of the "large sinkhole," its measurement was taken and the determination of the water inlet velocities made. The detected sinkhole was also used for the test of spatial detection of groundwater flows upstream from the dam by the "misse- a- la- masse" method. Downstream from the dam, in the part of the riverbed near the dam, the bathymetric recordings of the bottom were performed, as well as the diving investigations and underwater video camera recording, along with the measurements of water outflow at the locations of the detected springs. In the meantime, the investigative drilling and corresponding investigations in the boreholes (video endoscopy, carotage, etc.) (Fig. 16.16) were performed. Four investigation boreholes were drilled. The locations of these boreholes were determined in succession, depending on the results of all previously performed investigations.

Fig. 16.16 Entrance to cavern at the depth of 133 m from an altitude 337 m a.s.l (video endoscopy)

In accordance with the progress of the investigation works, a large number of sodium fluorescein tracer tests were conducted (used more than 60 kg), during which the tracer was injected in the existing piezometers upstream from the dam, then in detected sinkholes, as well as into the newly drilled boreholes (Fig. 16.16). Also, very important are the tracer tests repeated several times in the large sinkhole.

The salt tracing test was also performed, as part of the system for real-time monitoring. A large quantity of the tracer was injected into the "large sinkhole". Investigations were also performed in all 4 special-purpose boreholes, existing piezometers, and the springs downstream from the dam. Finally, after drilling of all boreholes and the completion of the corresponding investigations in all 4 boreholes (Fig. 16.17), cross-hole geoelectric and seismic tomography were conducted between the boreholes.

The results of all special-purpose investigations were necessary to perform such investigations as these:

- geodetic surveys in which the results were used for geodetic surveys of the contours of the dam, terrain, and structures in the surrounding area, as well as the survey of the storage bottom and riverbed bottom downstream from the dam in the zone of springs and all other spatial data,
- geological investigations in which the geological data were used for gathered from all available results of performed investigations (surface mapping, core mapping, analysis of tectonic, etc.),
- investigation drillings in which the details of the drilling method, geological data, geophysical carotage investigations, WPT investigations and video endoscopy,
- geophysical investigations in which the results were used for investigations performed by the geoelectrical scanning method, self-potential method, "misse- a- la- masse" method, cross-hole, geoelectric tomography, cross-hole seismic tomography, and measurements of electrical resistance on samples from boreholes, and
- hydrogeological investigations in which the results of investigations in the sinking zones upstream from the dam were used for determination of groundwater flow directions, measurements of discharge velocities, and measurements of groundwater levels.

All those data and results can be presented schematically as on Fig. 16.17.

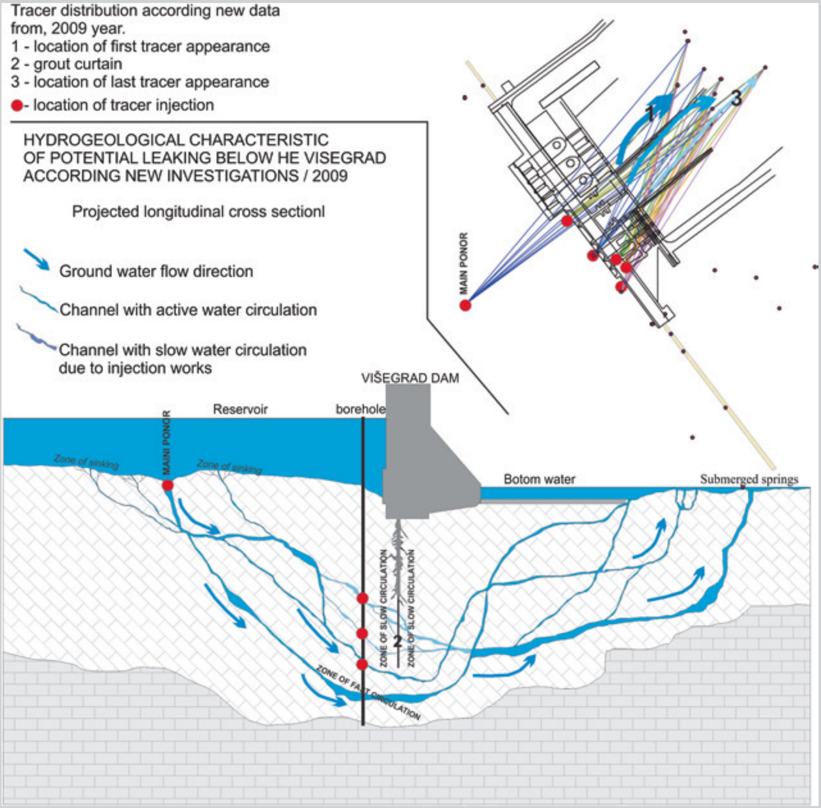

Fig. 16.17 Schematic longitudinal cross sections with conduit distribution. Layout tracer test results (S. Milanović, 2009 Report on special investigation on dam site Višegrad, Inst. for Develop. of Water Resources "Jaroslav Černi", Belgrade, unpublished)

Based on the above problem statement, it was safe to assume either that interactive work or integrated use of known 2D and partly defined 3D parameters is sufficient to produce an output of a three-dimensional conduit defined as 3D physical model. This case example presents certain investigations performed especially for the needs of the possible establishment of karst conduit genesis and spatial position below dam site (Fig. 16.18). The new data collected during grouting works give us evidence that the method which was applied for the construction of a 3D geometrical (or physical) model and parametric model of karst aquifer, aided by an incomplete data series, is feasible.

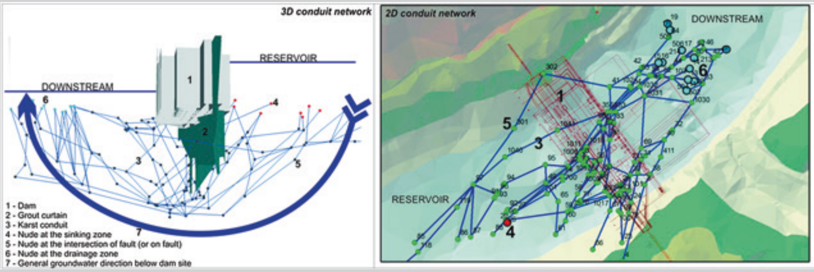

Fig. 16.18 2D conduit network of possible leakage pathways below dam site (model result; *right*); 3D conduit network of possible leakage pathways below dam site (*left*)

16.2 Karst Aquifers and Mining: Conflicts and Solutions

Veselin Dragišić

Department of Hydrogeology, Faculty of Mining and Geology, University of Belgrade, Belgrade, Serbia

16.2.1 Introduction

Numerous deposits of solid minerals (bauxite, polymetallic ores, skarn, etc.) are associated with karstified rocks. These rocks constitute the immediate overburden or basement, or both, of many ore deposits. In certain cases, the karstified rocks themselves are the mineral resources that are being mined. Groundwater from karst aquifers can be a major nuisance, threatening the mining operations with which they come into contact. This is especially true of underground mining, where ore is extracted from far below the water table. In advertent, intersecting of major karst conduits, due to a lack of knowledge about the hydrogeological conditions prevailing in the immediate environment, often leads to inrushes of groundwater into mining operations. A mine can be flooded over a very short time, causing human casualties and considerable loss. Additionally, intensive drainage of a karst aquifer can lead to subsidence and caving of the ground surface.

It is often difficult to predict water inflows to mining operations due to nonhomogeneous karstic character. In addition to water wells on the ground surface, mine drainage is provided by a combination of drilled drains leading out of the mining operations, drainage galleries, and drainage shafts.

One of the issues that mines in a karst environment have to cope with is the transformation of karst groundwater quality. Specifically, in carbonate karst, high-quality low-TDS groundwater transforms into highly acidic mine water, whose uncontrolled flow affects the quality of the immediate environment.

Operations involving evaporite extraction and drainage are faced with special problems. Extremely rapid karstification can lead to sudden groundwater discharges, often with immeasurable consequences.

16.2.2 Hydrogeological Types of Ore Deposits in a Karst Environment

More than 40 different types of ore deposits have been associated with karst. Also, the karstified rocks themselves can constitute mineral resources, such as limestones, marbles, calcareous tuff, sulfate rocks (gypsum-anhydrite), chloride rocks (halite and sylvite), and other rocks prone to karstification (Dublyansky and Nazarova 2004). The diverse ore deposits found in karst include bauxite, non-ferrous metals (Ni, Sb, Hg, Zn, and Cu), manganese, iron, and oil shales (Lunev et al. 2004). Uranium deposits have also been associated with carbonate rocks; in Uzbekistan and the USA, there are large deposits of this radioactive element in caves, caverns, enlarged conduits, and fractures (Bell 1963). Ore deposits in karst occur as mineral ore accumulations in contemporary karst depressions (ravines, sinkholes, and poljes), at the points of contact between carbonate rocks and igneous intrusives. The third type includes ore deposits overlain by younger sediments (Ford and Williams 2007b).

The positions of the ore deposits and mining operations relative to the water table are of special significance for the magnitude of inflow and the preferred drainage method. These deposits can be found in the vadose zone or the saturation zone in karst. Additionally, some ore deposits in karstified rocks, under the influence of a karst aquifer, are covered with younger sediments. Apart from these, ore deposits in coastal areas are distinguished because of the special way in which the inflow is formed. Evaporite deposits constitute a separate group due to a number of specific features.

16.2.2.1 Ore Deposits in the Vadose Zone

In general, mining operations above a karst aquifer are characterized by low and sporadic water enrichment. Intermittent pit water inflows occur solely after heavy rainfall. Dewatering of these mines does not pose a significant problem. One of the specific features of this type of ore deposits is the formation of perched aquifers, especially in bauxites (Box 16.2.1).

Box 16.2.1

Case Study—Bauxite deposits watering
Bauxite deposits near the City of Nikšić (Montenegro) are a typical example of ore deposits in the vadose zone. The bauxites are inter-stratified within carbonate formations (between Jurassic and Upper Cretaceous or between Lower and

Upper Cretaceous strata). Water inflows occur solely after heavy rainfall. High karstification of underlying limestones and a considerable depth to groundwater relative to the ore deposits enable direct infiltration of atmospheric precipitation in transit to the deeper reaches of the carbonate formation (Vasiljević et al. 1988). However, the bauxites in this part of Montenegro have a significant hydrogeological function. Being semipermeable rocks, they separate karstified overlying rocks from karstified underlying carbonate rocks. They form small (and the only) groundwater reservoirs in this part of the Montenegrin karst (perched aquifers). In certain localities, the aquifers are drained via perched springs, whose minimum discharge in places is as high as 1.0 l/s (Fig. 16.19). The significance of such springs is considerable, given that they occur in a typical karst environment, where springs are very rare while the demand for groundwater is high (Korać and Kecojević 1988; Radulović 2000a).

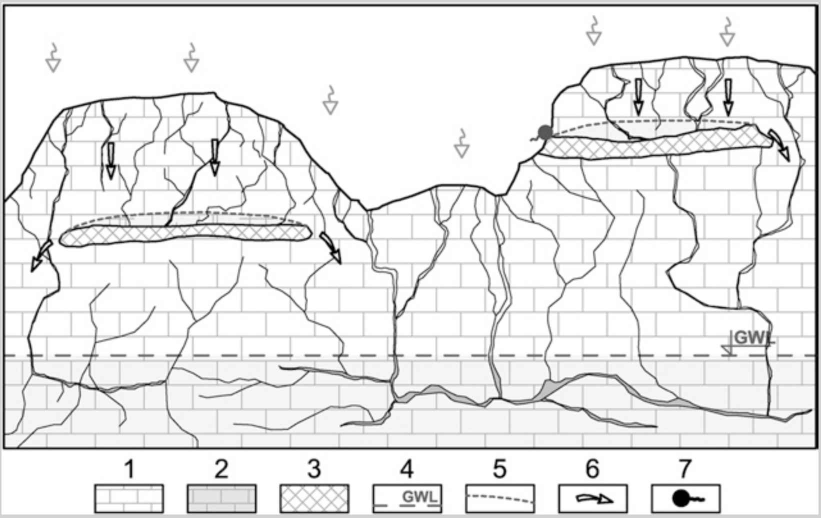

Fig. 16.19 Ore deposits in the vadose zone. *Legend 1* karstified limestone (vadose zone); *2* karstified limestone (saturated zone); *3* ore body (bauxite); *4* general groundwater level; *5* perched aquifer groundwater level; *6* groundwater direction; and *7* perched spring

16.2.2.2 Ore Deposits in the Saturated Zone

A large number of ore deposits are found below the water table in karst. They feature high groundwater inflow rates, which often hinder ore extraction, particularly underground mining. The ore is deposited within carbonate rocks, where the karst aquifer is unconfined (Fig. 16.20). The aquifer is recharged by infiltration of precipitation and water from surface streams. Bauxite deposits in the Urals, Russia, and lead and zinc deposits in Mirgalimsai, Kazakhstan, are found within a several hundred meters thick formation of karstified carbonate rocks (Ershov et al. 1989).

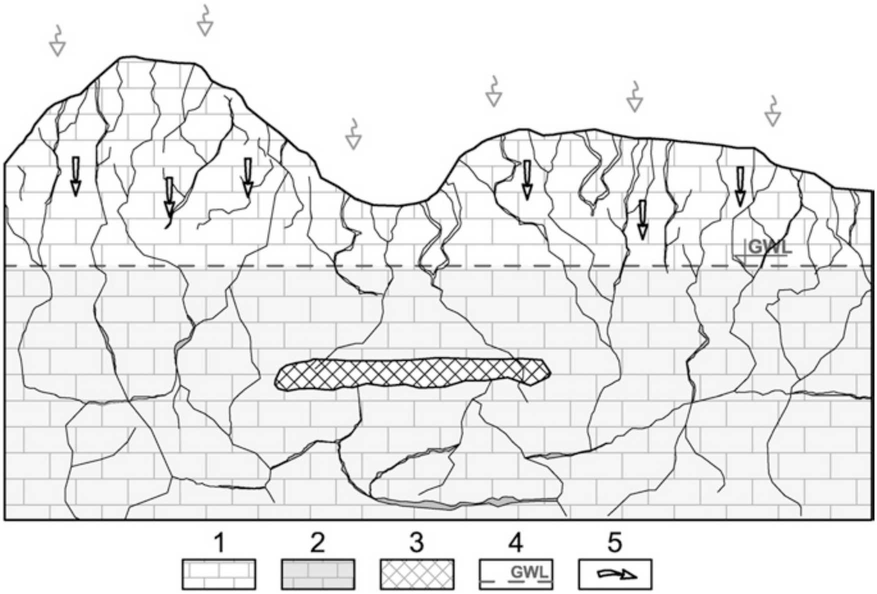

Fig. 16.20 Ore deposits in the saturated zone. *Legend 1* karstified limestone (vadose zone); *2* karstified limestone (saturated zone); *3* ore body (bauxite); *4* groundwater level; and *5* groundwater direction

They feature extremely high inflow rates: about 9 m^3/s in the Urals (Kleiman 1982; Plotnikov and Roginec 1987) and up to 3.3 m^3/s at Mirgalimsai (Kleiman 1982). Apart from underground operations, high inflow rates have also been recorded in opencast mines, such as in the Estonian oil shale deposits between karstified Ordovician dolomitic limestones, during periods of snowmelt and heavy rainfall, when they were as high as 3.0 m^3/s (Abramov and Skirgello 1968).

16.2.2.3 Ore Deposits on a Karst Bedrock Covered with Younger Sediments

Many ore deposits worldwide occur on a karst bedrock, which subsequent sedimentation processes have covered with younger, generally semipermeable strata. The groundwater is for the most part pressurized, and the inflow rates are extremely high. For example, the inflow rates to the Fan Gezhuang coal mine in China, from underlying karstified Ordovician limestones, are as enormous as 34 m^3/s (Gongyu and Wanfang 2006).

The bauxite deposits in Hungary north of Balaton, in the Halimba and Nyrad districts, directly overlie water-bearing Triassic and Jurassic limestones and dolomites, which are 500–600 m thick. Upper Cretaceous or Eocene and Pleistocene non-carbonate semipermeable formations lie discordantly over the bauxite deposits. The groundwater in most of the deposits is pressurized. The amounts of water pumped from the karst aquifer were rather impressive in the early 1980s, about 5 m^3/s, with a drawdown of 120 m (Alliquander 1982).

Box 16.2.2

Case Study—Confined karstic aquifer

The Maoče Coal Mine in the Pljevlja Coal Basin, Montenegro, is a good example of how pressurized groundwater can affect the inflow rate. The coal seam either overlies Middle Triassic limestones directly, or there is a transition marked by a thin bed of clay sediments (Nikolić and Dimitrijević 1990). A confined karst aquifer underlies the coal seam. Immediately after drilling, a borehole (BM-159) issued about 120 l/s at the point of artesian flow (Figs. 16.21 and 16.22). As a result, the capacity of some karst springs was reduced or they ran completely dry (Radulović et al. 1987; Radulović 2000b).

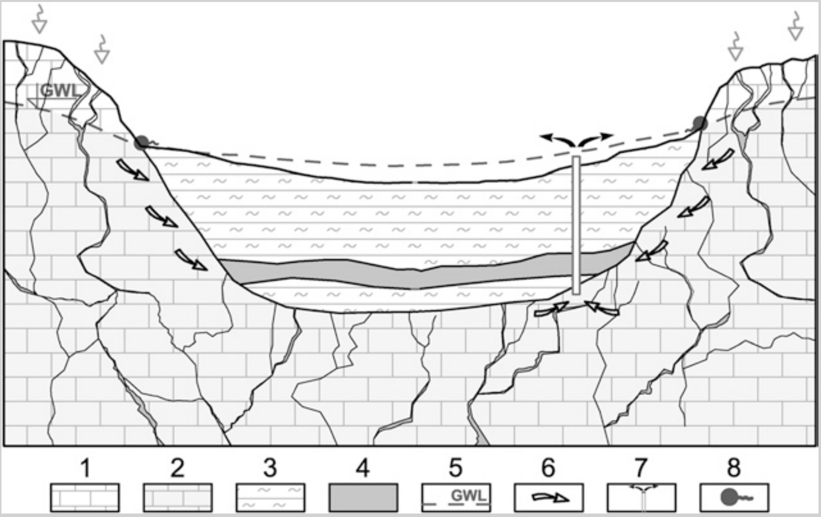

Fig. 16.21 Ore deposits over a karst bedrock, covered with younger sediments (Pljevlja Coal Basin, Montenegro). *Legend 1* karstified limestone (vadose zone); *2* karstified limestone (saturated zone); *3* Neogene sediments; *4* coal; *5* groundwater level; *6* groundwater direction; *7* exploration well; and *8* spring

Fig. 16.22 Artesian flow from exploration well BM-159, limestones in the background (Courtesy of Mićko Radulović)

16.2.2.4 Ore Deposits in Coastal Areas

Inflow rates to ore deposits in coastal areas can be boosted by seawater intrusion. Examples of this include the Raša Coal Mine (Croatia) and lead and zinc mines in Sardinia (Italy). The coal seams at Raša directly overlie Upper Cretaceous limestones. Drainage of the mining operations removed about 0.3 m^3/s of groundwater on average. Seawater intruded into the mining operations, which were as deep as 250 m below sea level (Šarin and Tomašič 1991).

At the Iglesias Lead and Zinc Mine, the ores are extracted from deposits located within a karst aquifer, 100 m below sea level. The karst groundwater is recharged by both atmospheric precipitation and seawater, such that high pumping rates caused seawater intrusion into the mining operations (Carta et al. 1982).

16.2.2.5 Evaporite Deposits

Evaporite rocks (salt and gypsum-anhydrite) are highly soluble and often form karst features that are generally found in limestone and dolomite deposits. A specific trait of evaporite karst, compared to carbonate karst, is that karst features are created rapidly, within several days, weeks, or years, while those in carbonate rocks need years, decades, or centuries (Johnson 2004).

Salt rocks are particularly prone to karstification under the influence of groundwater that is not saturated with chlorides. Low-TDS groundwater from other aquifers flows to the salt rock deposits, dissolving them and creating diverse karst features. The springs that naturally drain the karst aquifer remove a large amount of salt and deplete the deposits (Korotkevich 1970). Groundwater discharges through the newly created features in the ore deposits (caverns and caves) have often flooded mining operations (Abramov and Skirgello 1968).

Mining of evaporite deposits, primarily salt deposits, has produced numerous examples of subsidence and caving. There are two well-known cases of subsidence as a result of salt extraction: the Bereznikovsky Salt Mine in the Perm region of Russia and the salt mines in Cheshire, England (Ford and Williams 2007b).

Caving can also occur when not evaporites, but other deposits in their vicinity are mined. One example is the Gays River Mine in Canada. Lead and zinc ores are deposited in limestones covered with gypsum-anhydrite rocks, overlain by fluvio-glacial sediments. The drawdown within the ore deposits, due to the high solubility of gypsum-anhydrite rocks, resulted in subsidence and caving of the ground surface, as well as elevated rates of groundwater inflow to the mining operations. Despite numerous attempts to prevent the inflow, the rates increased from 100 to 250 l/s. This rendered mining unprofitable, and the mine was eventually shut down (McKee and Hannon 1985).

Box 16.2.3

Case Study—Collapse in salt mine area

In 1986, the potassium salt mine at Bereznikovsky in the Perm region of Russia experienced caving of gigantic proportions. It was caused by freshwater from 350-m-thick clastic sediments above the salt deposits, which reached the deposits and proceeded to destroy them. The inflow rates to the mining operations began to increase in January, when they were about 15 l/s, and reached more than 500 l/s on the night of 8/9 March. The mine was flooded. Within a few months, the mining operations of about 15 million m^3 became submerged. A large cavity was created above the mine, whose volume was in excess of 1 million m^3. The ground surface collapsed on the night of 25/26 July. The sink was ellipsoid on the surface, with 40×80 m sides, and about 170 m deep. Subsequent caving increased the sidewalls to

220 × 150 m (Fig. 16.23). The water table of the newly created pond (sink) was initially at about 100 m, but later rise to 60–70 m below the ground surface (Andreychuk 1996).

Fig. 16.23 Bereznikovsky Sink (Perm region, Russia)

16.2.3 Groundwater Inrush into Mining Operations

Groundwater inrush is frequent in mining of ore deposits in a karst aquifer environment. They are generally a result of insufficient hydrogeological exploration and a lack of preventative drainage measures. The results are very rapid flooding of the mining operations, substantial losses and, at times, human casualties. Such occurrences can be a consequence of different relationships between the ore deposits and the karst aquifer. Contrary to the carbonate karst, inrushes into evaporate karst are associated with intensive dissolution of the deposits under the influence of freshwater inflow, generally from overlying formations.

The brown coal mine at Vrdnik on Fruška Gora Mt. (Serbia) is a good example of how a lack of knowledge about hydrogeological circumstances can be devastating. Drilling of an exploratory pit in 1929 caused an inrush of some 500 l/s (water temperature 34 °C), resulting in flooding and abandoning of the mining operations. The sudden inflow occurred when mining operations passed through semi-permeable Tertiary sediments and entered underlying karstified Triassic limestones (Luković 1939).

Intensive drainage of a karst aquifer during the course of mining, without prior dewatering, has been one of the most frequent causes of groundwater inrushes in the past. For instance, at the bauxite mines in the Urals, at about 100–150 m below the ground surface, 93 inrushes were registered in 25 years. The highest measured inflow rate was 1.2 m^3/s (Abramov and Skirgello 1968).

Sudden intrusion of karst groundwater into mining operations can also be a result of heavy precipitation and rapid infiltration into the karst. For instance, the underground bauxite mine at Trobukva in West Herzegovina (Bosnia and Herzegovina), experienced several inrushes (0.18 m^3/s in 1982 and 0.5 m^3/s in 1987), caused by heavy rainfall (Slišković 1984; Bilopavlović 1988).

A hydraulic contact between surface water and karst groundwater is another potential cause of inrushes into mining operations. Operations at a dolomite quarry (in Pennsylvania, USA) cut through a karst conduit at a depth of 40 m, which was connected with surface water. Some 0.6 m^3/s of water from the conduit intruded into the mining operations (Lolcama 2005).

Box 16.2.4

Case Study—Sudden inrush from isolated aquifer

An atypical inrush of karst groundwater occurred in 1980 in the brown coal mine at Lipov Deo, belonging to the Senj-Resava Mines (Serbia). The inflow was caused by exploratory adit N-9 at an level of 327 m, penetrating the roof of a coal seam comprised of red Permian sandstones, which were only 2 m thick, and entering water rich Jurassic limestones (Fig. 16.24). The limestones, along with the Permian sandstones, were tectonically positioned so that they formed the roof of the coal seam. The initial inflow rates were 50 l/s, but after 6 days of continuous discharge, the mining facilities were flooded. Maximum inflow rates were about 170 l/s, but they later decreased to 20 l/s and were about 1.5 l/s in the next 1981 (Fig. 16.25). This pattern suggested an isolated karst aquifer whose recharge was very slow (Miladinović and Dragišić 1998; Miladinović 2000).

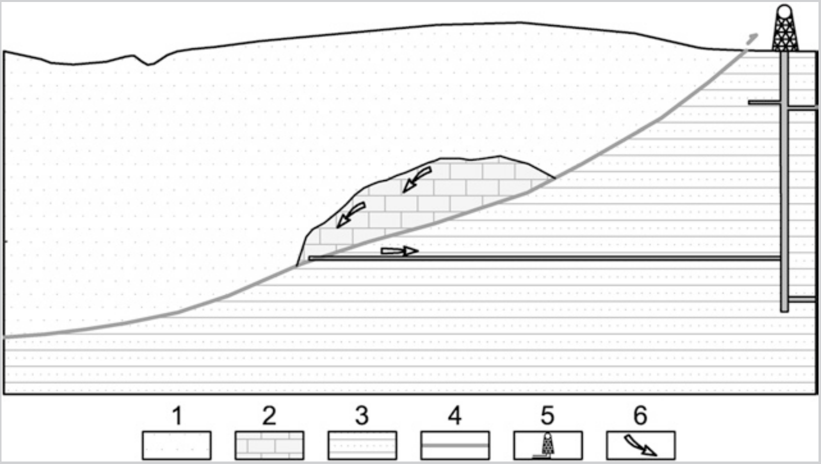

Fig. 16.24 Section of exploratory adit N-9 at the Lipov Deo Coal Mine (Serbia). *Legend* *1* Permian sandstones; *2* Jurassic karstified limestone (saturated zone); *3* Neogene sediments with coal; *4* overthrust; *5* shaft; and *6* groundwater direction

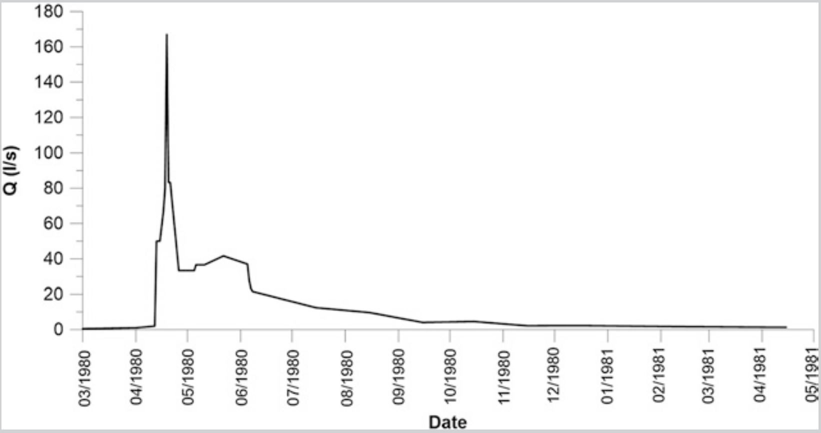

Fig. 16.25 Karst groundwater discharge hydrograph at adit N-9 of the Lipov Deo Coal Mine (Serbia)

16.2.4 Dewatering of Ore Deposits in a Karst Aquifer Environment

Safe mining in a karst aquifer environment requires efficient and timely drainage, or the prevention of pit water inflow (Table 16.2). In practice, a series of measures are implemented to dewater mining operations in a karst environment, depending on the type and size of the ore deposits, the inflow rate, the extent of karstification, hydraulic connection between groundwater and surface water, economic drivers, and similar parameters (Plotnikov and Roginec 1987). Drainage methods generally include the following: drainage wells on the ground surface; drilled drains leading out of the mining operations; drainage galleries and shafts; grouting of karst conduits; grout curtains; re-alignment of surface streams; tamping of ponors and river channels; and the like (Kleiman 1982). Due to the highly diverse nature of groundwater flow, lowering of the water table inside the deposits by means of a special configuration of wells is often not effective enough, so it tends to be combined with underground drainage works.

Table 16.2 Extreme karst groundwater inrushes into a number of mines worldwide (historical data)

Country	Mine	Mine product	Type of operation	Water inflow (m^3/s)		Reference
				Reg.	Max.	
China	Fangzhuang	Coal	Underground		34.2	Wenyong et al. 1991
					33.0	Gongyu and Wanfang (2006)
Hungary	Transdanubian region	Coal and bauxite	Underground and open pit	12.5		Kleiman (1982)
Hungary	Transdanubian region	Bauxite	Underground	5.0		Alliquander (1982)
Russia	Northern ural	Bauxite	Underground		9.1	Kleiman (1982)
						Plotnikov and Roginec (1987)
France	Region var	Bauxite	Underground		4.2	Tilmat (1973)
USA	Friendsville mine (Pemsilvania)	Zn	Underground	1.7	3.8	Kleiman (1982)
Kazakhstan	Mirgalimsai	Pb–Zn	Underground	2.7–3.3		Kleiman (1982)
Estonia	Estonian mines	Oil shale	Open pit		3.0	Abramov and Skrigello (1968)
Poland	Olkusz mine (3 mines)	Pb-Zn	Underground		7.3	Motyka and Czop (2010)
Poland	Lubin-Glogow	Cu	Underground	1.0		Bochenska et al. (1995)

Prior dewatering plays an important role because it ensures safe access to the ore deposits. It is commonly undertaken by means of drainage wells (water table lowering boreholes), located in water rich zones, in combination with drainage galleries and other works. One example of effective prior dewatering is the Olkusz Lead and Zinc Mine (Poland), which is one of the European mines that feature the highest inflow rates. The ore bodies are found in paleokarst dolomite cavities, at a depth of 200–300 m. The dolomites are overlain by a thick sequence of water-bearing Quaternary sands that store large amounts of groundwater and are hydraulically linked with a karst aquifer. Prior to extraction, the water table was lowered by means of wells and drainage galleries under each horizon (Ford and Williams 2007b).

Bauxite and coal deposits in Hungary, in an environment of Mesozoic water-bearing limestones and dolomites, are drained by galleries and large-diameter wells (shafts). In the early 1980s, the pumping rate was 5 m^3/s and the drawdown was 120 m (Alliquander 1982). The diameters of the drainage wells were 1.35–2.95 m, and each well was equipped with three submersible pumps (Tóth 1982).

Mine drains are generally drilled in cases where the karst aquifer to be drained overlies or is located to the side of the mining operations. At the Velenje Coal Mine in Slovenia, for example, such a system drains a karst aquifer in Triassic dolomites and limestones, which had caused several groundwater inrushes in the past, two of which were disastrous in 1918 and 1973 (Mramor 1984).

One of the measures undertaken to reduce groundwater inflow to mining operations is grouting of fractures and caverns, which constitute the greatest barriers in underground mining. Karst conduits are often exposed to high water pressures, destructive turbulent flows, and enormous inflow rates. Groundwater inflow is usually very fast and rates often measure hundreds or even thousands of l/s (Milanović 2000b).

This method can be effective but surprises are not rare. A typical example of ineffective grouting is the previously mentioned Trobukva Bauxite Mine in West Herzegovina (Bosnia and Herzegovina). Following a groundwater inrush and flooding of the pit in 1982, the karst conduits, which constituted the main groundwater pathways, were grouted between 90 and 240 m, section of decline. Water inflow rates in underground mining works decreased significantly, to amount of 2.5–12.0 l/s during the year. This water inflow prevention method had been cited as an effective underground bauxite mine drainage solution in the Dinaric karst of Herzegovina (Slišković 1984). However, a sudden inrush of more than 500 l/s in 1987 contradicted previous claims (Bilopavlović 1988).

The dolomite quarry in West Virginia is another example of ineffective grouting. The largest bitumen grout curtain in the North American karst was emplaced there to prevent river water inflow through karst conduits. However, a new karst conduit developed parallel to the stratification planes and river water continued to intrude into the mining operations (Lolcama 2005).

High drainage rates sometimes result in large-scale regional drawdown, as registered in the Lubin-Glogow copper mining region at depths of 600–1,200 m, where inflow rates from a karst aquifer in limestones and dolomites measured about 1.0 m^3/s. The drawdown extended over a surface area of 2,500 km^2 (Bochenska et al. 1995).

When evaporite deposits (primarily those of halite and sylvine) are dewatered, most of the groundwater needs to be evacuated before it gets into contact with the highly soluble ore deposits. For example, at the Solotvyno Salt Mine (Ukraine), “fresh” groundwater flows from an alluvial aquifer through fractures, destroying the salt rocks and creating karst features. This in turn boosts groundwater inflow and floods the mining operations. The task in such a mine is to undertake prior dewatering and prevent freshwater from reaching the ore deposits. Storm water also needs to be evacuated away from the deposits in good time (Abramov and Skirgello 1968).

As mining developed, mining methods were optimized and conventional mining gave way to solution mining, where ore deposits are dissolved by injected freshwater (Ford and Williams 2007b).

Ore extraction and mine drainage in a karst environment involve many risks. Apart from inrushes and contamination of karst groundwater, the most frequent adverse effects are subsidence and the creation of sinks on the ground surface and landslides in opencast mines.

High ore deposit/mine drainage rates result in dramatic drawdowns and subsidence. Possibly, the worst incident occurred in 1962 in South Africa, where intensive drainage of a karst aquifer in dolomites and limestones overlying gold deposits caused an ore preparation facility at the Dreifonte in Gold Mine to collapse. Twenty-nine people perished (Ford and Williams 2007b).

As a result of bauxite mine drainage in the northern Urals, a 500–600 km^2 cone of depression was formed on the ground surface. Karst-suffusion processes triggered by high drainage rates led to the development of more than 1,000 sinkholes, considerably enhancing infiltration of precipitation (Plotnikov 1989).

Box 16.2.5

Case Study—Landslides in contact zone

Depending on its position relative to the ore deposits, karst groundwater can have an adverse effect on rock stability of the ore deposits and thus be a threat to mining safety. The copper mine at Veliki Krivelj in eastern Serbia is an example of how karst groundwater causes landslides in opencast mining operations. The copper deposits are of the porphyry type, created in hydrothermally altered igneous (kaolinated and chloritized) rocks. These rocks, along with the ore deposits, are in tectonic contact with the Jurassic limestones of Veliki Krš Mt. (Fig. 16.26). Pressurized karst groundwater intrudes into the surrounding rocks, as corroborated during the course of drilling of exploratory adits within the deposits and surrounding rocks, as well as by chemical analyses of the groundwater (Dragišić and Stevanović 1984; Stevanović et al. 1991; Dragišić 1992; Stevanović and Dragišić 1995). A lack of timely drainage caused large-scale landslides (Fig. 16.27).

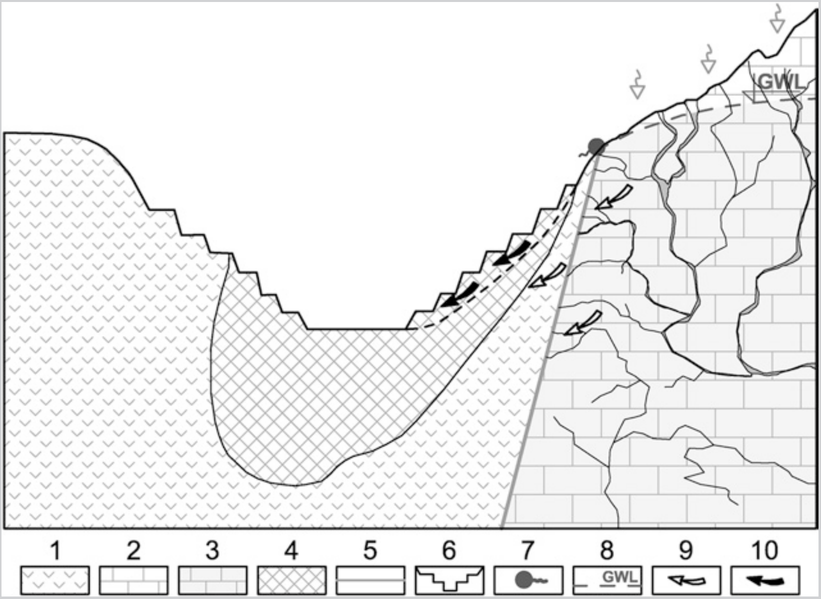

Fig. 16.26 Hydrogeological section through porphyry copper deposits at Veliki Krivelj (Serbia). *Legend 1* andesite (hydrothermal alteration); *2* karstified limestone (vadose zone); *3* karstified limestone (saturated zone); *4* copper deposit; *5* fault; *6* open pit; *7* spring; *8* groundwater level; *9* groundwater direction; *10* landslide

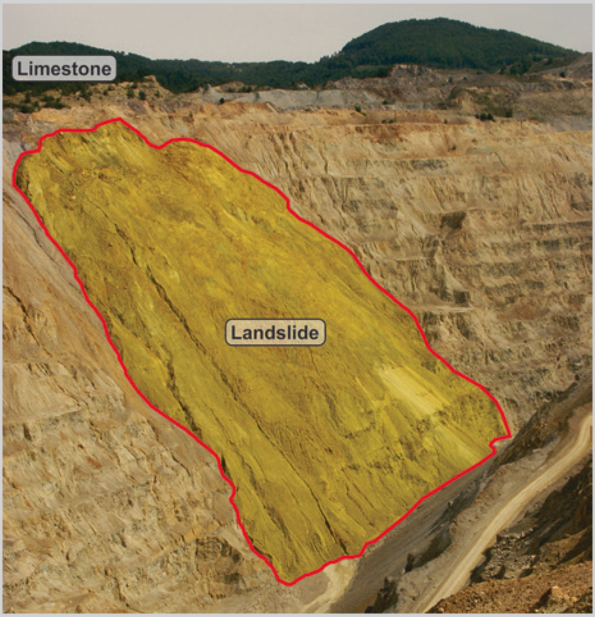

Fig. 16.27 Landslide at the opencast mine of Veliki Krivelj (Serbia)

16.2.5 Transformation of Karst Groundwater Quality

Ore extraction and high mine drainage rates in a karst environment often alter the quality of karst groundwater. This especially applies to non-ferrous ore deposits (such as those of Cu, Pb, Zn, Sb, and Hg), but is associated with other ores as well.

Prior to reaching mining operations, the quality of karst groundwater is generally good and such water is often used for drinking water supply, irrigation, and other needs. Since the discharge rates are frequently high (several hundreds or even thousands of liters per second), the significance of such groundwater cannot be overstated. Consequently, in order to use karst groundwater for practical purposes, it needs to be tapped before it comes into contact with mining operations. There are numerous examples of karst groundwater use. The quality of the groundwater pumped from the bauxite deposits in Hungary is very high, such that this water is used for drinking water supply (Alliquander 1982).

An 8-km-long drainage gallery in the lead mine at Homesford (USA) taps some 870 l/s, of which 460–580 l/s is used for drinking water supply (James 1997). Several hundred liters per second of high-quality karst groundwater, tapped before it reaches lead and zinc mining operations at Mirgalimsai in Kazakhstan, is used for drinking water supply and irrigation of farmland (Plotnikov and Roginec 1987).

As karst groundwater flows into mining operations, it comes into close contact with the ore and other minerals that make up the ore body. As a result of complex geochemical processes, generally high-quality karst groundwater of the HCO_3-Ca type, with a pH level of 7–7.5 and TDS < 1,000 mg/l, becomes transformed into the SO_4-Ca type, with low pH and high TDS levels and elevated concentrations of Fe, Al, and other elements. A typical example of such transformation are the copper mines at Veliki Krivelj and Majdanpek in eastern Serbia, where the inflow is formed from karst aquifer discharge or at locations where tailings and waste rock dumps have been formed on karst (Dragišić 1992; Dragišić 1994; Stevanović and Dragišić 1995).

A special type of karst groundwater transformation is encountered under the influence of high-TDS seawater in coastal areas. Namely, high pumping rates at mining operations in such areas lead to over-pumping of low-TDS groundwater and intrusion of high-TDS seawater. Typical examples are the lead and zinc mines in Sardinia (Carta et al. 1982) and the Raša Coal Mine in Croatia (Šarin and Tomašič 1991).

Box 16.2.6

Case Study—Groundwater quality transformation
The Kizelkovsky Coal Basin in the Perm region of Russia is a classic example of karst groundwater quality transformation. The stone coal seam is Lower Cretaceous, emplaced between carbonate rocks. Accompanying minerals include pyrite, calcite, siderite, and gypsum. Underground coal extraction began more than 200 years ago, reaching depths up to 1,000 m below

the ground surface. The mine has been abandoned because of uncontrolled water discharges from 12 pits, which created a major environmental issue. During the course of coal extraction, underground mining formed a drain for karst groundwater discharge from the carbonate cover. The mine pits in this region were among those with highest water inflows in Russia. The pits were abandoned and flooded in 1990. However, groundwater of transformed quality is still being discharged from the karst aquifer overlying the coal seam (Fig. 16.28). The transformed groundwater is typical acidic mine water (Bankovskaya and Krasavin 2004; Maksimovich 2004).

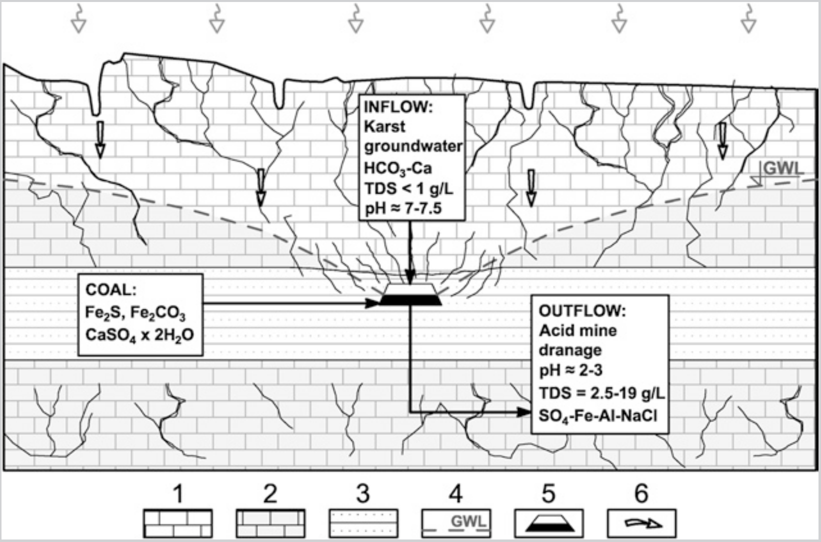

Fig. 16.28 Schematic representation of the formation of acidic mine water at the Kizelkovsky Coal Mines. *Legend 1* karstified limestone (vadose zone); *2* karstified limestone (saturated zone); *3* clastic sediments with coal; *4* groundwater level; *5* mining works with mine water; and *6* groundwater direction

The transformation process can be summarized as follows: There is a karst aquifer in the roof made up of non-carbonate rocks with coal, in highly fractured and karstified limestones, whose thickness in places is more than 1,000 m. The limestones are partially exposed and heavily recharged by infiltration of atmospheric precipitation. The quality of the karst aquifer groundwater is excellent. The aquifer provides drinking water supply to the extended area of the mine (Bankovskaya and Krasavin 2004). After the mining operations were abandoned, the pits that served as karst groundwater drains became flooded. The geochemical processes that take place in coal mining operations in the presence of water and accompanying minerals (pyrite, siderite, gypsum, etc.) tend to create acidic mine water (Lovell 1983; Lottermoser 2007; Dimitrijević 2013).

The mine water is typical acidic water of the SO_4–Fe–Al–Na–Ca type. TDS generally measures 2.5–19.0 g/l, but in certain cases as much as 35 g/l. The pH levels are up to 2–3. Compared to low-TDS water, such mine water features a number of times higher concentrations of lead, copper, zinc, silver, nickel, cobalt, and other minerals (Maksimov 2004).

When the morphological conditions are favorable, the mine water is gravitationally discharged untreated, from the pits to the ground surface. One of the pits is the Kalinin Mine from which acidic mine water flows to a nearby river (Figs. 16.29 and 16.30).

Fig. 16.29 Gravitational discharge of acidic mine water from the Kalinin Mine

Fig. 16.30 Flow of acidic mine water to the river (Kalinin Mine)

16.3 Remote Techniques for the Delineation of Highly Karstified Zones

Milan M. Radulović

Faculty of Civil Engineering, University of Montenegro, Cetinjski put bb, 81000 Podgorica, Montenegro

16.3.1 Introduction

The majority of karst terrains are characterized by a high degree of heterogeneity. The results obtained by applying methods for assessment of local karstification (e.g., borehole tests) often cannot be reliable to extrapolate to a wider area. The use of remote sensing provides the opportunity to assess the spatial distribution of karstification in the subregional scale. Analysis of satellite and aerial images allows identification of geomorphological and tectonic forms that may indicate the highly karstified zones. There are several factors that indicate the karstification, and which can be mapped by remote sensing, and this contribution is focused on two of them: surface karstification (K_{sf}) and density of faults (T_f). By overlapping maps of these two factors using geographical information system (GIS) techniques, the final map expressed through a *KARST* index is obtained. The application of this approach provides an image of the spatial distribution of karstification, even for areas that are inaccessible for direct field research. The obtained map can be used as a basis for solving some of engineering problems in karst that are related to the regulation of water, extraction of groundwater, and protection of karst aquifers from contamination.

16.3.2 The Complexity and Categorization of Karst Terrains

The complexity of karst terrains, and often inaccessibility for direct field observations, induce a need for application of remote sensing, as one of the additional methods for karst research. The observation of karst terrains from a distance, except obtaining a more general image of study area, provides an opportunity for indirect delineation of zones with different degree of karstification, which is the main objective of the approach described in this section. Application of the mapping approach is shown on the example of catchment area of Karuč springs (Montenegro, Dinarides; Fig. 16.31).

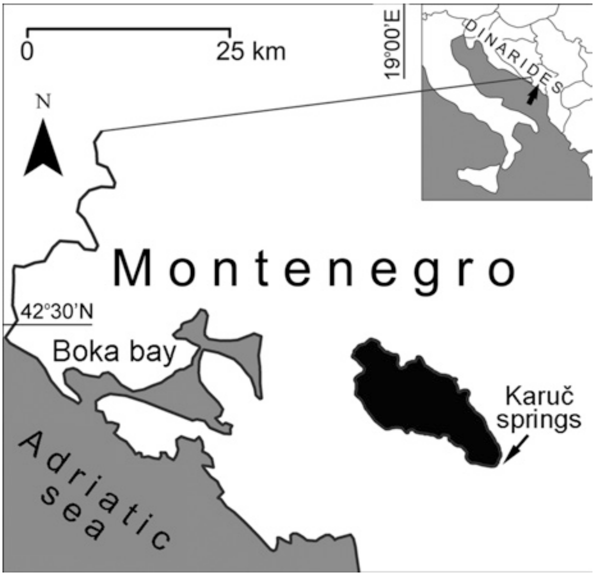

Fig. 16.31 Location of Karuč springs catchment area

For the purposes of categorization of karst terrains, different criteria have been used by different authors. In most cases, when considering the regional scale, the categories have been delineated according to the distribution of karst landforms such as sinkholes and caves (*number of sinkholes*/km^2, *area of sinkholes*/km^2, *volume of sinkholes*/km^2, *number of caves*/km^2, *length of caves*/km^2, and *volume of caves channels*/km^2). There are also some examples of satisfactory mapping of karstification through a so-called sinkhole index, which is based on the mean spacing of closed contours in a given area (Gregory et al. 2001).

The results of various tests (pumping test, slug test, Lugeon test, and packer test) and geophysical loggings (borehole televiewer, caliper logging, electromagnetic induction logging) give excellent data about local porosity and karstification, but the problem is the limitation of the results only on a narrow area around the tested borehole. A number of field geophysical methods can also provide an image of karstification, but for the analysis of a complete catchment area that are often partly impassable, these methods also appear to be impractical. In recent years, airborne electromagnetic (AEM) techniques for remote mapping of karstification have been developed (Smith et al. 2005; Supper et al. 2009; Gondwe et al. 2012). These techniques are especially suitable for wider areas. Their application gives an image which shows electrical conductivity anomalies that are mainly related to surface karst landforms (Smith et al. 2005). However, these methods are still under development, but they will likely play an important role in the future to address this issue. Also, it is interesting to note airborne and satellite thermal imaging sensors which have been used for detecting temperature anomalies. Temperature anomalies could occur in the opening of the caves due to the difference in outside air temperature and the temperature of air that outflow from the caves (Zurbuchen and Kellenberger 2008; Wynnea et al. 2008). Furthermore, underwater karstification, precisely the locations of vruljas, where colder groundwater discharge below the level of sea or lake (Figs. 16.32 and 16.35), could be detected by using thermal imaging sensors.

The approach presented in this section consists of analysis of satellite and aerial images in order to identify geomorphological and tectonic forms that are often indicators of highly karstified zones. The procedure of mapping is extracted from the more complex KARSTLOP method which is used for assessing the spatial distribution of recharge of karst aquifers (Radulović et al. 2012). Two subfactors, that can be mapped using remote sensing, are extracted from the aforementioned method. These subfactors are the surface karstification (K_{sf}) and the density of faults (T_{f}). Through them, by using GIS techniques, the final map of the karstification assessed by remote sensing techniques (*KARST*) index is obtained. The *KARST* index represents the index that indirectly reflects the degree of karstification.

The possibilities of application and some limitations of the presented approach are also discussed in this section.

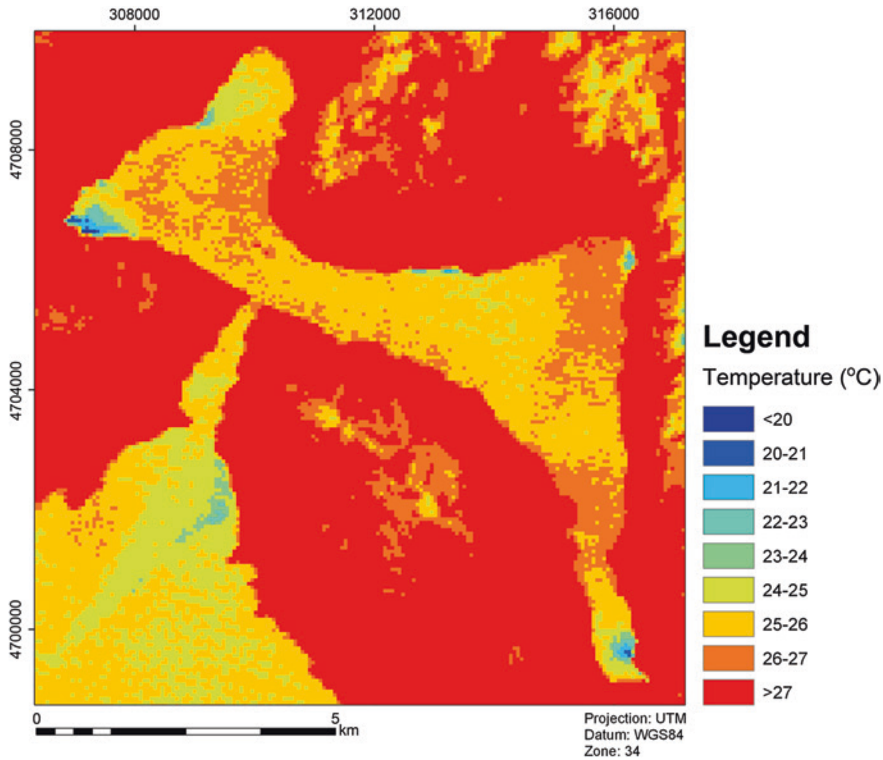

Fig. 16.32 The map of sea temperature in the Boka bay (Montenegro) which obtained by satellite image LANDSAT 7 ETM+ (thermal infrared band–Band 6; resolution 60 m; date of capturing: June 23, 2002). The temperature anomalies (*blue tones*) indicate the locations of the submarine springs where colder groundwater discharges below the sea level

16.3.3 The Concept of Mapping of Karstification by Using Remote Sensing and GIS

This subsection presents the approach for obtaining the map of karstification, which has been developed and applied to highly karstified terrains of External Dinarides. There are two factors that indicate the degree of karstification, and which can be mapped from satellite and aerial images. Those are factor K_{sf} (surface karstification) and factor T_{f} (the density of faults).

16.3.3.1 Map of Surface Karstification

Special attention, when analyzing the degree of surface karstification, should focus on the analysis of the distribution of surface karst landforms. The surface karst landforms are recognizable on aerial and detailed satellite images, such as Quick

Bird and SPOT (resolution about 2.5 m). Also, consideration should be given to an appropriate scale in which the map of surface karstification will be created (preferably between 1:25000 and 1:100000).

A coverage of karst terrains with sinkholes and uvalas can sometimes reflect the degree of karstification, since they are often elongated along the faults which were additionally extended by corrosive actions of water. A distribution of sinkholes is, from many authors, accepted as a criterion for categorization of karst terrains (Gregory et al. 2001; Angel et al. 2004). The problem is that sinkholes are in large numbers mainly formed on the karst plateau, but they rarely occur on steep slopes which were formed by later erosion. For this reason, the use of density of sinkholes as the only criterion does not give a complete image of the degree of karstification. There are karst terrains where sinkholes are totally absent, while other indicators (karren fields, caves, and fluctuation of discharge) suggest a high degree of karstification.

Since the karren fields are often the only karst landforms on the slopes, it is reasonable that one criterion for mapping the surface karstification is an area of karren fields (or degraded zones) per 1 km^2 and that the second criterion is an area of karst depressions (sinkholes, uvalas, poljes, and dry valleys) also per 1 km^2. By overlapping input maps created by these two criterions, a map that will satisfactorily show the degree of surface karstification can be obtained. According to this conception, the highly karstified terrains would be areas with uvalas and sinkholes, whose slopes are scarred by karren.

So there are two subfactors, K_{sf1} (area of degraded zones/km^2) and K_{sf2} (area of karst depressions/km^2), according to which the categorization of karst terrains is performed (Table 16.3). Limit values between the categories are defined by measurements on a number of sites along the External Dinarides.

Factor of surface karstification (K_{sf}) represents the average of subfactors K_{sf1} and K_{sf2} (Table 16.3).

Figure 16.33 shows some of the karst terrains that could be the subject of mapping according to the described concept. The first image (Fig. 16.33a) shows the karst terrain with poorly expressed surface karst landforms, from which karst depressions and karren fields are almost totally absent. The second image

Table 16.3 The categorization of karst terrains according to the subfactors K_{sf1}, K_{sf2}, and according to the factor K_{sf}

Area of degraded zone (karren fields, ruin-like relief, etc.) per unit square (10^3 m^2/km^2)	K_{sf1}	Area of karst depressions per unit square (10^3 m^2/km^2)	K_{sf2}	$K_{sf} = (K_{sf1} + K_{sf2})/2$
<60	1	<25	1	1
60–120	2	25–50	2	>1–2
120–180	3	50–75	3	>2–3
180–240	4	75–100	4	>3–4
>240	5	>100	5	>4–5

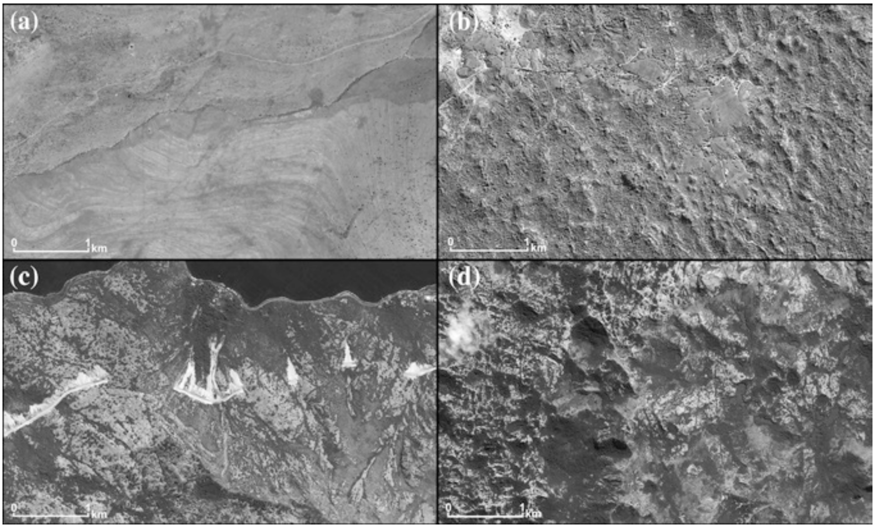

Fig. 16.33 Satellite images of karst terrains **a** terrain with poorly expressed surface karst landforms; **b** terrain with karst depressions but without degraded zones; **c** karst slope where the karren fields are well developed; **d** terrain where karst depressions and karren fields are together

(Fig. 16.33b) shows the karst terrain on which karst depressions (sinkholes and uvalas) are very common, while degraded zones are poorly represented. The third image (Fig. 16.33c) shows a karst slope where the karren fields are well developed, while sinkholes and other karst depressions are completely absent. Finally, the fourth image shows (Fig. 16.33d) the terrain with a high degree of karstification, where there are both karst depressions (sinkholes and uvalas) and karren fields.

16.3.3.2 Map of Fault Density

Karst landforms, especially karst channels, are often elongated along the faults. Intersections of two or more faults represent zones with a greater chance for the existence of caves. For this reason, it is considered that is reasonable to introduce a map of fault density as one of input maps for assessing the degree of karstification. Map of fault density (T_f) sows contours which are categorized according to the length of faults per unit of surface (km/km^2). Before the creation of this map, it is necessary to create a digital map of fault lines. The Landsat 7 ETM+ satellite images (resolution of 30 × 30 m), after appropriate processing, can be a good basis for creating the map of fault lines. Karstic terrains of Dinarides are generally photogenic for the analysis and interpretation of images (Pavlović et al. 2001), so that the degree of subjectivity in identifying faults is significantly lower than in the analysis of other terrains.

Table 16.4 The categorization of terrains according to the density of faults

Density of faults (km/km^2)	T_f
0–1	1
1–2	2
2–3	3
3–4	4
>4	5

Table 16.5 The categorization of karst terrains according to the value of the *KARST* index

Karstification	*KARST* index
Very low	2
Low	>2–4
Moderate	>4–6
High	>6–8
Very high	>8–10

Production of a map of fault density is greatly facilitated by the use of appropriate software for spatial analysis. The contours of the map of fault density are obtained based on the categorization shown in the Table 16.4.

16.3.3.3 Karstification Map

The *KARST* index is obtained through the two previously described factors (K_{sf} and T_f). It represents the degree of karstification which is assessed by geomorphological and tectonic analysis of satellite and aerial images. The *KARST* index is calculated by adding the factors K_{sf} and T_f (*KARST* index $= K_{sf} + T_f$).

A *KARST* map is obtained by overlapping the map of surface karstification (K_{sf} map) and the map of fault density (T_f map), using appropriate GIS software. The result is a map that shows the spatial distribution of the *KARST* index, which ranges from 2 to 10. Higher values of the *KARST* index should correspond to highly karstified terrains, while lower values should be related to less karstified terrains built of less permeable carbonate rocks. The Table 16.5 shows the categorization of karst terrains according to the value of the *KARST* index.

Box 16.3.1

Case Study—Application to the catchment area of Karuč springs
The study area is located in the southeastern part of the Dinaric Alps, in the territory of Montenegro (Fig. 16.31). That is the catchment area of Karuč springs which occupies an area of about 116 km^2. The complete catchment area is built of carbonate rocks (limestones and dolomites). The soil is very

thin or completely absent. The catchment area of Karuč springs belongs to the geomorphological unit named "Old Montenegrin karst plateau," which is characterized by a large number of surface karst landforms (sinkholes, uvalas, poljes, and dry valleys).

The recharge of karst aquifer occurs primarily by precipitation (mean annual precipitation is about 2,700 mm). Hydraulic conductivity of the carbonate aquifer is relatively high. Groundwater flows mainly through privileged directions which are marked with faults and joints. Fictive velocity of groundwater flow, measured by artificial tracers, is from 0.65 to 5.40 cm/s (Radulović 2010). Discharge of karst aquifer occurs through sublacustrine springs (vruljas) that occur along the coastal part of the Skadar Lake (Figs. 16.34 and 16.35). The mean annual discharge of Karuč springs is 7 m^3/s.

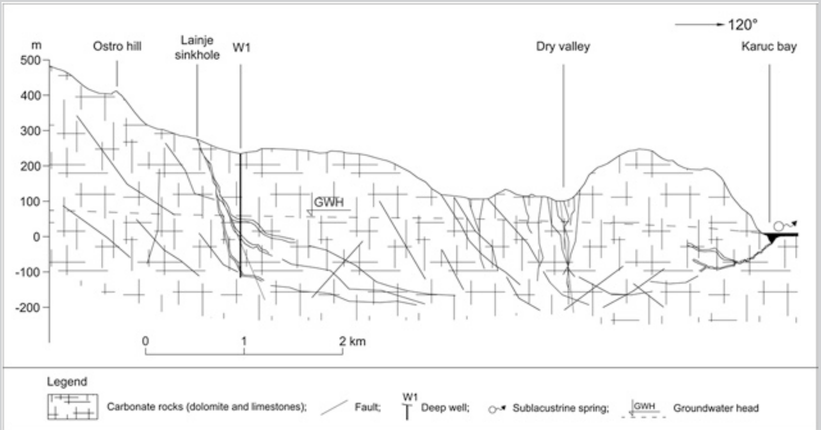

Fig. 16.34 Hydrogeological section of Ostro hill–Karuč bay (Skadar Lake)

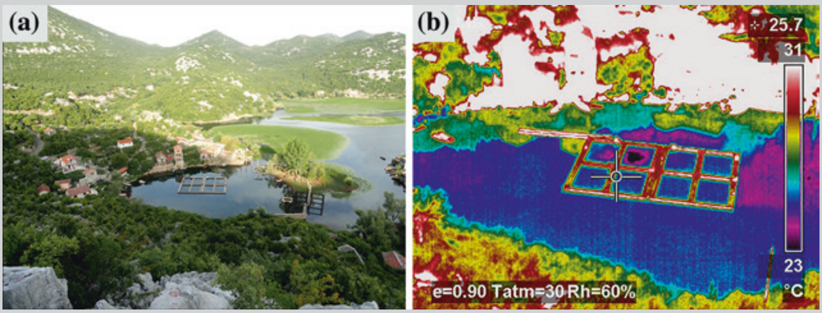

Fig. 16.35 **a** Photo of Karuč bay captured in visible spectrum; **b** photo of Karuč bay captured in thermal infrared spectrum, from which it can be seen the temperature anomaly (*purple tones*), i.e., the main location of groundwater discharge

***K_{sf}* map of Karuč springs catchment area**

As a basis for mapping the surface karstification, orthorectified satellite images (Quick Bird and SPOT images with a resolution of about 2.5 m), and aerial images (captured by photogrammetric camera WILD RC30 in the scale of about 1:5000) were used.

One of the first steps in the process of mapping the surface karstification has been the identification and mapping of surface karst landforms, so separately the map of karren fields and separately the map of the karst depressions have been drawn (Fig. 16.36a, b). From these two maps, the K_{sf1} and K_{sf2} maps have been obtained (Fig. 16.36c, d), and by their overlapping, the K_{sf} map has been created (Fig. 16.36e, f).

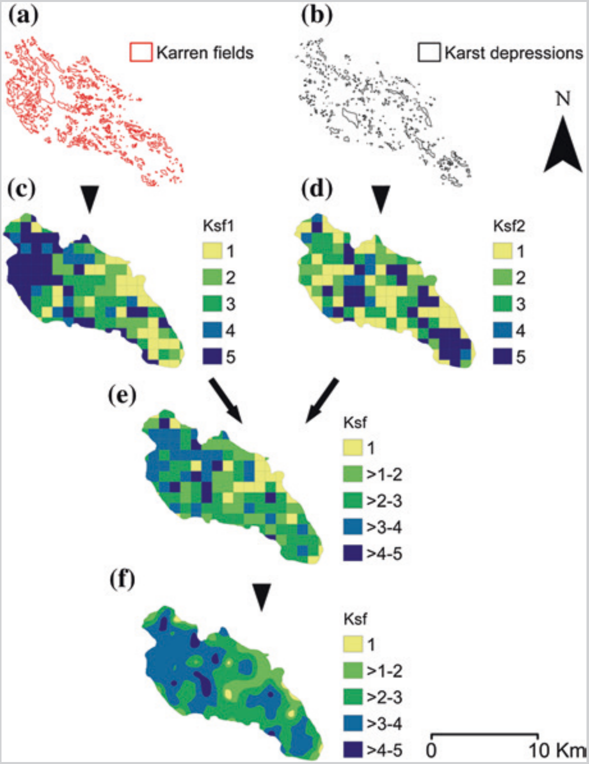

Fig. 16.36 Flow chart of procedure for derivation K_{sf} map. **a** Map of karren fields; **b** map of karst depressions; **c** K_{sf1} matrix map; **d** K_{sf2} matrix map; **e** K_{sf} matrix map; and **f** K_{sf} contour map (modified from Radulović et al. 2012). Springer and the Environmental Earth Sciences, 65(8), 2012, 2221–2230, A new approach in assessing recharge of highly karstified terrains–Montenegro case studies, Radulović MM, Stevanović Z, Radulović M, Fig. 2, Copyright 2012. With kind permission from Springer Science and Business Media

T_f map of Karuč springs catchment area

The map of fault lines has been obtained by the interpretation of Landsat ETM+ color composite image created from bands 4, 5, and 7, which is considered as one of the most suitable for geological research (Won-In and Charusiri 2003). The images have been previously processed in order to enhance their quality. Enhancing contrast of raw images has been performed by selective linear transformations of the original pixel values.

Based on the digital map of fault lines (Fig. 16.37), by applying previously presented categorization (Table 16.4) and using ArcGIS 10.1 software (Line Density tool), map of fault density of Karuč springs catchment area has been obtained (Fig. 16.38).

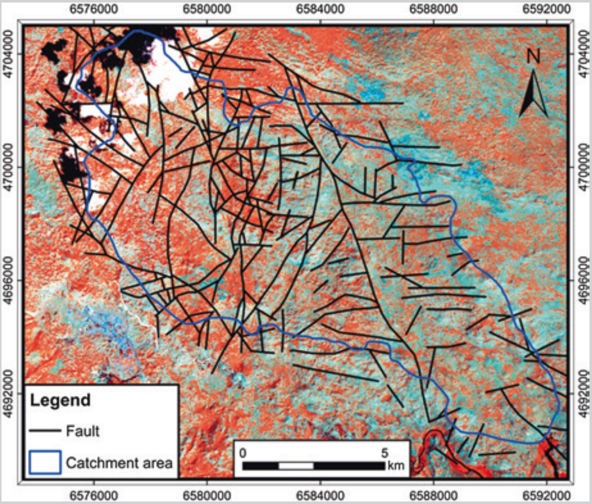

Fig. 16.37 The map of fault lines of Karuč springs catchment area (the background image is LANDSAT ETM+ color composite created by bands 4, 5, and 7)

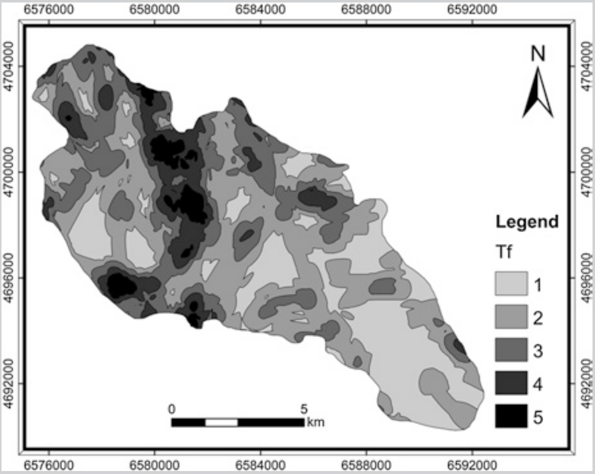

Fig. 16.38 The map of fault density of Karuč springs catchment area

The map of the KARST index

The map of the *KARST* index is created by overlapping K_{sf} and T_f maps, adding the values of these two factors and categorizing obtained contours according to the Table 16.5.

From the map (Fig. 16.39), it can be seen that the highly karstified terrains, i.e., areas with an increased *KARST* index, are represented in the northwestern part of the study area. Also, from the map, it can be seen that the terrains that are assessed as less karstified are represented in the central and southeastern parts of study area. Terrains that have been classified in the category of moderate KARST index occupy the largest surface on the catchment area of Karuč springs.

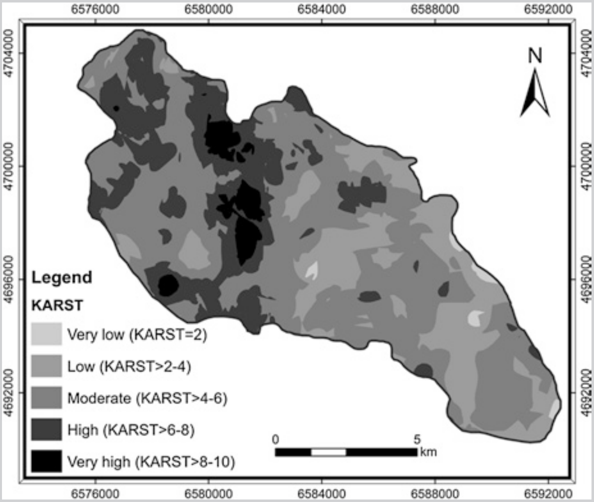

Fig. 16.39 The map of the *KARST* index of Karuč springs catchment area

16.3.4 Discussion

For the first time, the mapping approach has been applied to the catchment area of Karuč springs (Montenegro). The proposed approach allows simple mapping of karst terrains according to the degree of karstification, but it is only the assessed image that can significantly deviate from the real state. Large discrepancies could be expected especially in the case of deeper karstification. By this approach, it is only possible to identify the areas where caves could be expected, but the real axis of cave channels cannot be determined. The map of the *KARST* index more reliably indicates the degree of shallow karstification, which has been developed to the depth of a few tens of meters.

After preparation of the final map, in order to verify the assessed degree of karstification, visits of some parts of the mapped area have been done. On the most visited sites, the assessed degree of karstification by using remote sensing mainly matches the subjective assessment from the field (Fig. 16.40). Therefore, assessed degree of karstification by using remote sensing mainly matches to the field assessment of shallow karstification.

Maps obtained by the presented concept are the most desirable to create in the early stages of research. Thus, the research can focus on potential areas with increased karstification, which would be checked by applying geophysical methods and exploratory drilling on the field.

The presented approach has its advantages and disadvantages. Some of which are shown in the Table 16.6.

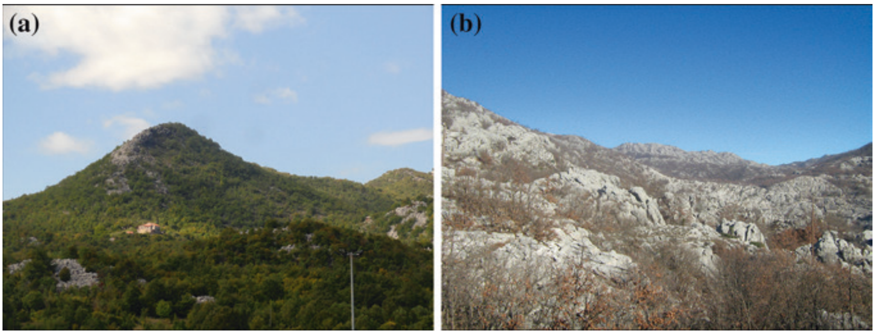

Fig. 16.40 **a** Terrains of the southeastern part of the mapped area which have been assessed (by remote sensing) as low to moderate karstified; **b** terrains of northwestern part of the mapped area which have generally been assessed (by remote sensing) as highly karstified terrains

Table 16.6 The advantages and disadvantages of the presented approach

Disadvantages	Advantages
There may be certain errors (interpolation errors, errors in analysis and interpretation of satellite images)	Maps are produced without major investments of funds
Obtained maps, due to the limited details, are not especially reliable for the analysis in the local scale	The result is spatial distribution of karstification that is not possible to obtain by applying most of the other methods
Maps are not especially reliable for the assessing the karstification of deeper zones, but are mainly intended to assess shallow karstification	The results are also obtained for inaccessible karst areas, where it is not possible to perform the conventional on-site investigations
It is not possible to obtain quality maps for the areas covered by vegetation	The maps are obtained based on easily available data (aerial and satellite images)

16.3.5 Conclusion

Preparation of the map of karstification by using remote sensing represents a relatively easy way to delineate highly karstified zones in the regional scale.

The map can be used as an additional base for solving some of the engineering problems in karst. For example, it could be used for assessing suitability of the terrain for the construction of reservoirs (in terms of permeability), for identifying potential sites for the abstraction of groundwater, for identifying sites for artificial aquifer recharge, as one of basis for the modeling of groundwater flow in the karst, as one of the input maps for mapping groundwater vulnerability, for a first assessment of suitability of the terrain for the construction of underground facilities, and as a basis for planning research in order for rationalization.

The approach needs to be tested on a greater number of karst areas in order to achieve additional improvements. The concept of mapping is adapted for highly karstified terrains, so it is important in the following stages to highlight the possible shortcomings and take eventual modification for the terrains with lower degree of karstification.

In the future, it is necessary to devote additional attention to this issue, considering the importance of the assessment of karstification for more complete research and protection of karst aquifers.

16.4 Combat Mixture of Groundwater and Surface Waters in Karst

Zoran Stevanović

Centre for Karst Hydrogeology, Department of Hydrogeology, Faculty of Mining and Geology, University of Belgrade, Belgrade, Serbia

16.4.1 Introduction

The mixture of fresh groundwater and surface water is a frequent problem in karst, and most problematic for the sustainable use of fresh groundwater. This problem results mostly from the high permeability and low attenuation capacity of karst aquifers, particularly those formed in open (unconfined) structures. The existence of such a mixture makes it complicated to distinguish and separate fresh groundwater from surface flows or water reservoirs such as a lake or sea. Even more problematic is the restoration of the natural quality of groundwater polluted by surface water flows or seepage, as discussed under the topic of remediation in Sect. 17.4 of this book.

Concerning the kinds of surface water and their negative impact on adjacent aquifers, surface water can generally be distinguished as follows:

1. Waste surface waters (already contaminated and untreated or partially treated, or leakage from various sources such as landfills, industry, communal systems; pollutant liquids may also be flowing through canals or be being stored in ponds in direct or indirect contact with karst),
2. Sea and brackish waters (saline to various degrees),
3. Lake waters (potentially polluted),
4. River waters (potentially polluted).

Regardless of which is present, it is always better to prevent their contact with karstic waters. Interventions may be very different and should be adapted to the concrete circumstances. Some of the remedial measures that may be applied in karst are as follows:

- making an impermeable seal along canal bottoms or riverbeds,
- building small dams or weirs,
- constructing grouting curtains,
- diverting surface waters to other directions and catchments,
- plunging ponors,
- making so-called reactive barriers by pumping additional freshwater into aquifer.

How to tap fresh groundwater in coastal karst and avoid the intrusion of surface, particularly saline, waters is the practical problem on which this discussion is further focused.

16.4.2 Historical Experience

Tapping coastal aquifers and distinguishing freshwater from seawaters are regularly a very difficult task. The Phoenicians constructed special structures such as collective boats with iron funnels and leather pipes to force freshwaters to flow upwards to the surface to supply their citizens. Freshwater was also tapped by tubes or specially constructed bells driven down spring outlets or amphorae turned upside down to catch the flow (Bakalowicz et al. 2003a).

Many cities in the Mediterranean basin, one of the World's cradles of civilizations, were built near large sources of freshwater (Stevanović and Eftimi 2010; Stevanović 2010a). An important role in this case was played by the position of impermeable barriers which dictate the drainage point to be below sea level or above it. Therefore, where this barrier is well above sea level, the chances to utilize freshwaters are increased and this was well known by the skilled Greeks and Romans who defined the position of many famous historical towns. For instance, on the eastern Adriatic shoreline (Dalmatian coast, Croatia), the town of Split (lat. *Spalatum*) was built in close proximity to the major karstic spring in the Jadro area which is around 30 m above sea level (see Fig. 2.4), and the town of Dubrovnik (lat. *Ragusa*) was built near the huge spring of Ombla which discharged at only 3 m a.s.l. Some other springs such as the Bistrica group of springs in Albania (including the famous Syri Kalter—Blue Eye, see Fig. 3.41) are envisaged as one of the potential sources even for transboundary distribution to southern Italy (Puglia Region) due to their huge minimal discharge and secure discharge points, some 50 m a.s.l. (Eftimi 2003). In the Adriatic basin, the main karstic aquifer system is from the Mesozoic age while the main barrier is represented by younger Eocene flysch. The deep and regional flow from inland is thus adapted to the regional erosion base as is the sea level (Fig. 16.41).

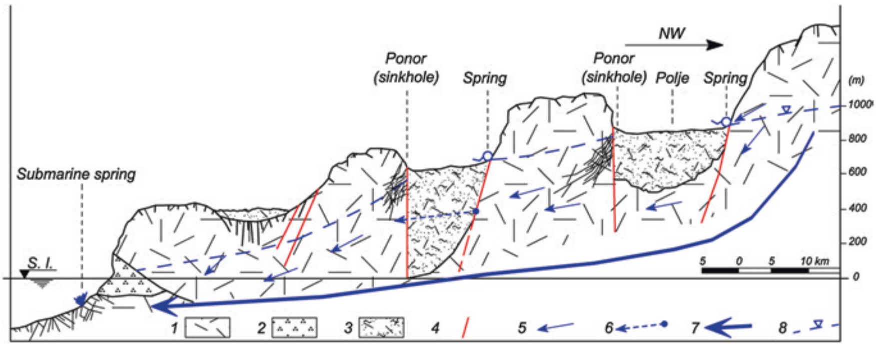

Fig. 16.41 Schematic typical cross section through the karstic poljes of the Dinarides (after Mijatović 1983, modified by Stevanović). *Legend 1* karstified Mesozoic limestone; *2* flysch barrier; *3* porous aquifer of polje; *4* fault; *5* groundwater flow; *6* direction of flow around the barrier; *7* regional flow; *8* groundwater table

During the geological history in Neogene and the Messinian salinity crisis, the connection between the Mediterranean Sea and the Atlantic Ocean was closed and the sea level in the Mediterranean basin declined by several hundred meters. As a result of intensive karstification and first a specific arid and then a glacial climate, many springs along the paleocoast were also opened at a lower position but today, with the sea level significantly raised, they are functioning as submerged springs. Therefore, the hydrogeological evolution of the Mediterranean littoral karst was decisively affected by the rise in level of about 100 m during the last interglacial state (Mijatović 2007).

In contrast to drainage points above sea level, the submarine springs (vruljas) occur in places where the impermeable barrier is missing or is much below the sea. Bakalowicz et al. (2003a), Fleury et al. (2007) and Dörfliger et al. (2010) emphasized that the location of many of these springs in the Mediterranean basin is relatively well known and documented. An overview of the largest submarine springs in the Mediterranean basin, but also in other regions with large submarine discharge (Florida, Caribbean basin, Black Sea, Persian Gulf, and Pacific islands), has been provided in an unpublished report by M. Bakalowicz (2014, Karst submarine and related coastal springs of the world. Report on WOKAM project, unpublished) for the ongoing World Karst Map project (WOKAM, in press).

16.4.3 *Hydraulic Mechanism and Methods to Identify Submerged Flows*

The classical Ghyben–Herzberg formula which defines the relationship and interface between fresh and salty water is generally valid for karst aquifer (Stringfield and LeGrand 1971; Bonacci 1987; Arfib et al. 2005), but its application, as in the case of Darcy law, should be used with caution (Fig. 16.42) because direct contact of two fluids established in saturated karstic channels and cavities and transitional zone of brackish water could be very much extended (Fig. 16.43).

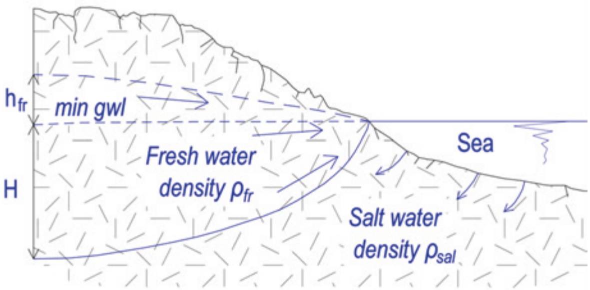

Fig. 16.42 Sketch for Ghyben–Herzberg hydraulic relationship

Fig. 16.43 Open structure of highly karstified rocks in direct contact with the sea. Porto Vromi (Zakhintos, Greece)

The hydraulic relationships are driven by the difference in water density between fresh and seawater, but the more important factor in this relation is the hydraulic head in the aquifer system (h_{sr}). The freshwater is of lower density (ρ_{fr}) and overlies saltwater (ρ_{sal}) as a lens. Consequently, when head (lens' thickness) is larger, the chances for mixture are reducing. Although the regime of karst aquifer regularly varies throughout the year, the same aquifer may discharge fresh or brackish, or even totally saline water and spring discharge is activated permanently or seasonally.

The Ghyben–Herzberg formula for depth of fresh—saline water interface can be calculated as follows:

$$H = \frac{\rho_{fr}}{\rho_{sal} - \rho_{fr}} h_{fr} \tag{16.1}$$

where,

H depth to interface fresh—saline water
ρ_{fr} density of freshwater
ρ_{sal} density of saltwater
h_{fr} freshwater head above sea (and minimal groundwater level)

Although the density of freshwater is 1.0 and the density of saltwater is 1.025, under hydrostatic equilibrium, the depth to the interface is 40 times the height of the water level above the sea. Consequently, one meter of drawdown of freshwater results in an intrusion of saltwater by 40 m and more. And more intense pumping will cause fast salinization of the aquifer.

The problem with the Ghyben–Herzberg hydraulic law is the assumption that there is no flow under hydrostatic equilibrium and that the head of freshwater

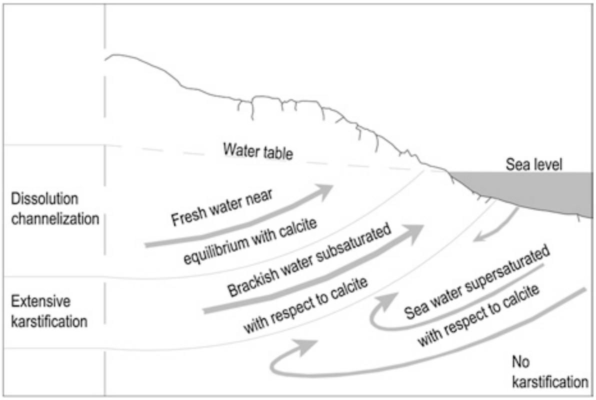

Fig. 16.44 Schematic model of different salinity zones in karst of Yucatan (After Beck, 1992)

comes to zero at the point of contact with the sea. Because the movement and discharge of fresh groundwater have to be taken into account and the interface is not sharp but transitional, many new formulae have been developed to overcome these deficiencies since the law was imposed in the early 1900s (Arfib et al. 2005).

The dynamic of coastal aquifer discharge and the problem of interface salty–freshwaters have been studied for many years and by many authors (Zektser et al. 1973; Mijatović 1983; Drogue and Bidaux 1986; Drogue 1996; Bakalowicz et al. 2003a; Fleury et al. 2007). A simple scheme is also presented by Back (1992) who studied the famous Yucatan karstic aquifer in Mexico (Fig. 16.44).

Box 16.4.1

Yucatan Peninsula (Mexico)—Open and vulnerable karst system

The Yucatan Peninsula aquifer, a huge open system at low altitude (average 30 m a.s.l.), consists of highly permeable limestones and rapid infiltration of rainfall but also discharges into the sea. However, when in some areas such as the city of Merida in the NW or the tourist center of Cancun, pumping of groundwater becomes intensive, the attained drawdown results in the intrusion of salty water inland as well as its movement upward. Back (1992) identified large hydraulic conductivity of karst and lack of freshwater head as reasons why a saltwater body underlies a freshwater body and is extended over almost one third of the peninsula's surface. The mixing zone between fresh and seawater is marked by brackish water whose salinity increases downward. Back (1992) states that a geochemical zone with increased salinity also stimulated the karstification process and this is why many cenotes such as karstic inlets (shaft-like sinkholes with extended saturated deep and long canals), lagoons, coves, and crescent bays are well developed particularly along the east cost of Yucatan (Fig. 16.45).

Fig. 16.45 Cenote in the middle of Yucatan, near Valladolid

Many cases of deterioration of littoral aquifers and deep intrusion of salty water have been noticed worldwide. Where there is absolutely no problem of salt intrusion, there is almost no littoral karst, at least during droughts or low water seasons. Particularly, problematic might be the situation in the islands where freshwater bodies are completely surrounded by seawaters.

Different methods are used in hydrogeological practice to identify the presence of deep groundwater flows in coastal zones in order to capture them before they reach the shoreline or start to mix with salty waters.

The reconnaissance or initial stage of survey of coastal aquifers includes remote sensing methods. A satellite image represents a digital signature of reflected electromagnetic energy. Images from a multispectral scanner include bands from different spectral areas: blue, red, green, infrared, etc. Analysis of the lithology, tectonic pattern, vegetation index, and moisture vegetation index can also be supported by careful observation of the shoreline and possible changes in the color or intensity of the reflected signal in surface water near the banks.

Besides optical locating of the sublacustrine springs, infrared thermography techniques, which are based on the detection of temperature anomalies, could also be applied. The temperature anomalies usually appear at locations where there are discharges of colder groundwater below the level of the warmer sea/lake water, i.e., at locations of submerged springs. But, the reverse situation of warmer groundwater discharging into colder seawater is also possible in some regions particularly in the Northern Hemisphere. Examples of identification of sublacustrine springs along the shoreline of Skadar Lake in Montenegro are explained in Sect. 16.3. The same section also presents the use of terrestrial recording by thermal infrared camera which may help in identifying submerged springs (see Fig. 16.35).

Different geophysical methods, including geoelectrical resistivity, spontaneous potential, mise à la masse, electrical tomography, very low frequency, microseismics, gravimetry, and geophysical logging, can be applied for defining groundwater flows (Arandjelović 1976). One very specialized method is induced polarization which was successfully applied for the first time in the Adriatic islands in the 1970s. This method helps to distinguish further caverns filled with water from caverns filled with clay, as both provide similar values of resistivity when an electrical resistivity method is applied.

Along with classical tracing tests which enable visualization of colored waters, different types of robots or underwater vehicles are constructed for identification and sampling of water. For example, the autonomous underwater vehicle, Taipan 1 and 2, has been developed in LIRMM laboratory (France) for measurements of conductivity and temperature values of water at certain depths as well as GPS positioning of sampling sites (Lapierre et al. 2008). It is a torpedo-shaped vehicle with a single propeller (very similar to a current meter), and relatively small in size (1.80 m length, 0.2 m diameter, 60 kg).

Thanks to this vehicle, specialized divers can enter saturated karst channels of large dimensions and collect valuable information on their extension as well as do water sampling (see Box 3.13). Mapping the karstic deep channels may significantly support engineering projects on aquifer regulation.

Finally, the exploratory drilling, the subsequent pumping test, and the hydrochemistry analyses provide the most precise data on groundwater flow, optimal discharge, and water quality which are essential elements when evaluating the relationship between fresh and salty water.

16.4.4 Sustainable Tapping and Use of Fresh Karstic Waters

According to Mijatović (1983), one of the main tasks of hydrogeological research is to distinguish the following:

- aquifers opened toward the sea,
- aquifers having an incomplete barrier (resulting in the presence of a wide range of salinity from brackish waters), and
- aquifers discharging over complete barriers.

The last are "safer" from seawater intrusion and provide the most convenient ambience for tapping and engineering regulation of aquifer. As already stated, in the case of the Mediterranean coast, the freshwater supply greatly depends on the barrier extension and local position.

During the last half century, many successful projects have been implemented in the Adriatic basin which solved the problem of increased water demands and pressures on already vulnerable coastal aquifers (Alfirević 1963; Mijatović 1984; Komatina 1984; Biondić and Goatti 1984; Milanović 2000c; Eftimi 2003; Biondić and Biondić 2003; Al Charideh 2007). Some of these are explained in *Hydrogeology of karstic terrains, case histories*, which is edited by Burger and Dubertret, and which is Volume 1 of the IAH series International Contributions to Hydrogeology (1984).

Similarly, the book *Groundwater management of coastal karstic aquifer* resulted from the project COST action 621 (2005) and contains discussions and results from 62 selected observation and studied sites from 8 Mediterranean countries. The aquifers are displayed in the four groups, class A (40 % of the total studied aquifers) being most vulnerable to salt intrusion due to unconfined character and high permeability. Classes A and B comprise almost 80 % of all studied aquifers "where salt intrusion is a real problem and over-exploitation is the common way to manage the aquifer."

Many attempts have been made worldwide to find an appropriate solution to tap freshwater from submerged springs. Some of them are based on previously described principles first applied by the Phoenicians. For instance, Bakalowicz et al. (2003b) described the function and result of testing of a tapping device constructed by the French company Nymphea water in the 1970s and improved in 2003. The secure cylinder enclosing the spring was designed to follow the seabed contour. The chimney is topped with a half sphere and pipe conveying water upward. The system relies on differences in density between spring water and seawater, and freshwaters are driven to the surface by the denser, more brackish water below.

Although any attempt to capture submerged freshwater flow is difficult and the final result is uncertain, the most appropriate solution is to tap fresh groundwater flow as far as possible from the sea and direct discharge zone. In many cases, the horizontal galleries placed directly into the conduit which enables gravity flow are a better option than pumping from drilled wells or shafts. But whatever intake is applied, systematic monitoring of discharges or pumping rate versus water salinity should ensure sustainable aquifer development and prevent the effects of water salinization or quality deterioration (Fig. 16.46).

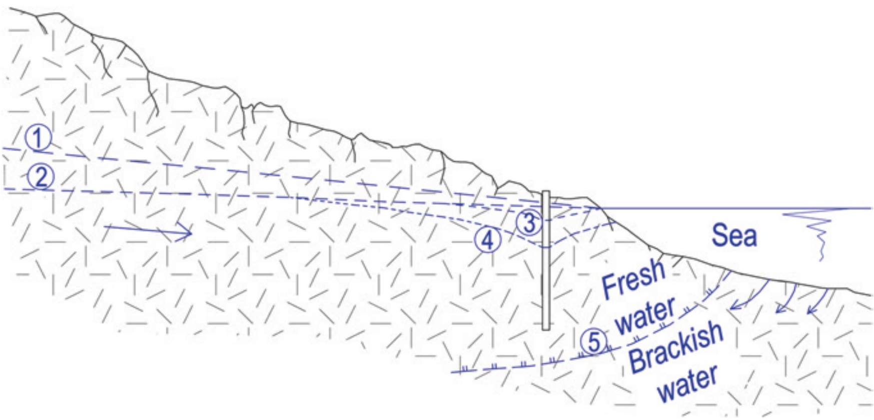

Fig. 16.46 Typical cross section in littoral karstic aquifer where pumping rate from drilled well has to be accommodated to actual hydraulic head. *Legend 1* Static water table in high water period, large hydraulic head prevent mixture of fresh with salty water; *2* Static water table in low water period, declined hydraulic head does not prevent mixture of fresh with salty water and a counterbalance is established; *3* A small pumping rate and radius of well are still feasible and slight increase in mineralization of tapped water is only possible. *4* A large pumping rate disturbs interface of fresh and salty water and intrusion of the latter is very probable. *5* Approximated zone delineates brackish and farther away salty water body from freshwater body. It is movable in accordance with status of hydraulic head (pressure in aquifer system)

Box 16.4.2

Ain Zeina, Lybia—saline water intrusion due to over-pumping

In order to improve the water supply of Benghazi (Libya), a proposal to tap Ain Zeina brackish spring water far from the coastal zone was provided by experts of the Geological Survey of Serbia (B. Mijatović, 2006, Geological and hydrogeological framework of integrated water resources management in Libya. Report. Geological Survey of Serbia, Belgrade, unpublished). Research undertaken in the Jebel Akhdar area resulted in 10 exploratory wells drilled in well-karstified numulitic Eocene limestones in the most prosperous zone of Sidi Mansur which is 11 km from the coast (Fig. 16.47). The yield of these wells ranged from just a few l/s to 20 l/s. More importantly, the Cl ion content was regularly lower than 400 ppm.

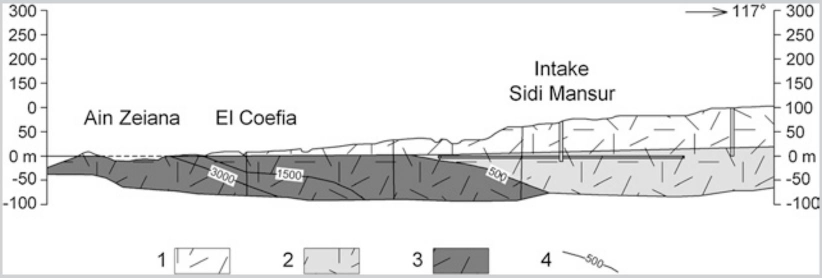

Fig. 16.47 Hydrogeological cross section of the Sidi Mansur (Jebel Akhdar)—Ain Zeina (modified from B. Mijatović, 2006, Geological and hydrogeological framework of integrated water resources management in Libya. Report. Geological Survey of Serbia, Belgrade, unpublished). *Legend 1* Unsaturated Eocene limestones; *2* Karstic Eocene aquifer with freshwater; *3* Karstic Eocene aquifer with brackish water; *4* Salinity iso lines, values in ppm

Based on these results, one vertical shaft with a long horizontal galley was designed and constructed (Fig. 16.48). It was the first horizontal gallery executed in Africa in modern times (B. Mijatović, 2006, Geological and hydrogeological framework of integrated water resources management in Libya. Report. Geological Survey of Serbia, Belgrade, unpublished).[1] The vertical shaft is excavated to a depth of 82 m. The bottom is at 1.9 m a.s.l. while the average groundwater table is at 3.5 m a.s.l. From the shaft bottom, the 500-m-long gallery is excavated perpendicular to the groundwater flow (2 × 250 m from the center of shaft). While the Ain Zeina spring discharged an average yield of 1,000 l/s of brackish water, the Sidi Mansur tapping structure enabled the pumping of 400 l/s (with a Cl content of 300–350 ppm).

Unfortunately, with no established proper monitoring and control over the extensive pumping from the shaft, the salinity front intruded further inland and the groundwater became brackish even in the Sidi Mansur. After 15 years of operation, the average groundwater salinity reached a value of 1,500 ppm.

[1] Collecting galleries were used for the water supply of ancient Cyrene (Cyrenaica) in Roman times.

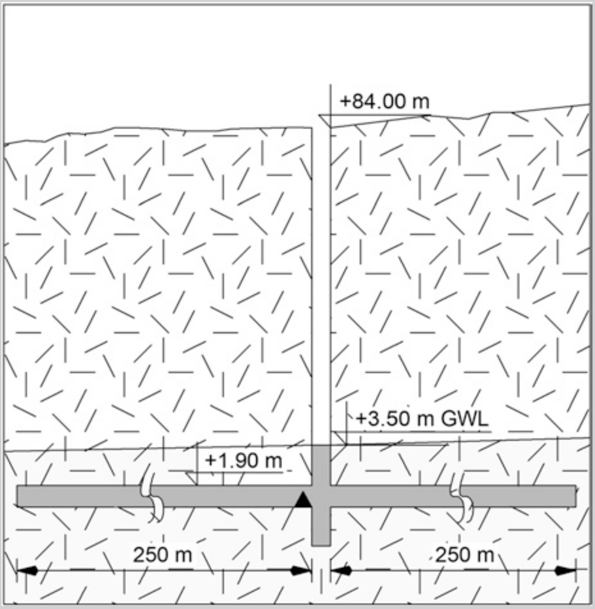

Fig. 16.48 Sidi Mansur tapping structure—vertical shaft and gallery (redrawn based on personal explanation of B. Mijatović)

Box 16.4.3

Port-Miou (France)—Regulation of brackish springs by underground dam
One of the world's most known projects in coastal karst is the intake and underground dam constructed for the city of Marseille with the aim to distinguish fresh and seawater flows. The two large springs, Port-Miou and Bestouan, are in fact underground drowned karst rivers issuing from the Calanques range of hills on the coastline between Marseilles and Cassis. They are discharging much more groundwater (3 m^3/s) than calculations from conventional formulae allow for and an apparent surface catchment of maximal 150 km^2. It has been assessed that only infiltration from a close alluvial plain fed by water from irrigation canals together with inflows from more distant limestone formations can cause such a huge discharge (Potié et al. 2005).

In order to find an appropriate response to the fast-growing water demands of the city of Marseilles, in 1964 two French institutions, the Geological Survey of France Bureau de Recherches Géologiques et Minières (BRGM) and a local water company from Marseille (SEM), conducted an extensive geological, geophysical, topographic survey including tracing tests and diving exploration (described also in Box 15.4.4 of Sect. 15.4). The survey of Port-Miou resulted in the construction of the first underground dam in 1972 and a complete closure of the gallery with a second underground dam (Potié et al. 2005). The objective of the phase-1 dam was to prevent saltwater intrusion without modifying the aquifer's pressure. The principle of a "chicane" dam was adopted. This involved building a pair of dams 530 m from the sea outlet: an upstream chicane dam on the gallery floor and a downstream chicane dam on the gallery roof (Fig. 16.49).

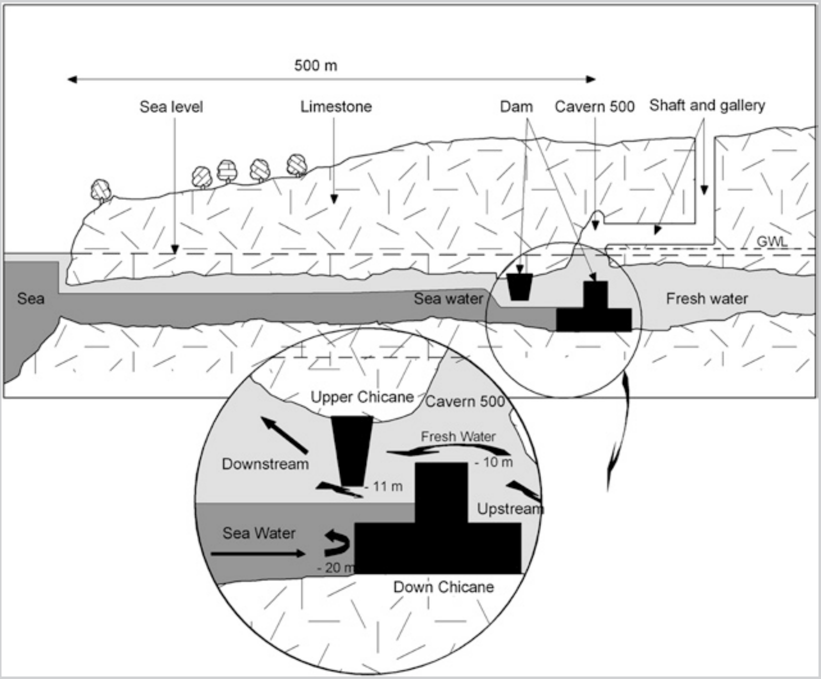

Fig. 16.49 Port Miou underground dams (after Potié 2005). The inverted dam forces freshwater downwards, while the dam on the gallery floor prevents saltwater from penetrating farther upstream into the exploitation gallery

Construction of chicane dams did not entirely stop salinization of groundwater, but it had a significant positive effect: Salinity of the water dropped from 4–5 to 2–3 g/l at the surface, and upstream of the dam at a depth of 20 m below sea level from 18–20 to 3–4 g/l. However, complete prevention of salinization was not possible.

There are also many sublacustrine springs or spring/seepage registered along the riverbeds which are not easy to tap and separate from surface waters. An example of very intense underground drainage along lake shores is the Skadar/Shköder Lake, the largest in the Balkans, shared between Montenegro and Albania. Only on the Montenegrian shoreline has the average groundwater flux from the submerged springs been estimated at more than 10 m^3/s. From this, one of the largest reservoirs of freshwaters in all of Europe, one recent project successfully conducted, has ensured the water supply of all Montenegrian ports and touristic cities on the coast (Stevanović 2010b). Experience collected from this project (Box 16.4.4) and a sophisticated solution to distinguishing lake and groundwater waters can also be accordingly applied at many other submerged springs along the lakes and Adriatic coast.

Box 16.4.4

Bolje sestre intake (Montegero)—Separated lake water and groundwater
The new Montenegro Regional Water Supply System (RWSS) covers the water supply of all municipalities along the coast. The RWSS is designed on a maximal capacity of 1.5 m^3/s; the total pipeline length is 140 km, of which the continental part from Skadar Lake to the coast comprises 33 km. This new system, functioning since 2010, has solved the acute problem of water shortage due to the small discharge of previously tapped coastal springs in summer months when the tourist season dictates maximal water demands.

The tapping of Bolje sestre sublacustrine spring was first proposed by Radulović (2000b) because of its shallow depths of submerged discharge points and its assessed sufficient and stable flow throughout the year. After conducting complex hydrological, hydrochemical, hydrogeological surveys, tracing tests, exploratory drilling, and identification of the position of the main groundwater transient channel, three options of tapping freshwater flow were evaluated (Stevanović 2010b):

1. by enclosing the area of the source discharge, and using a small coffer dam, the discharging water can be captured and pumped into the scheme;
2. custom-built metallic pipes can be jacked into the ground of the lake, and anchored by underwater cementation, creating intake shafts for pumping to the scheme,
3. a shaft of large diameter located on land, approx 5–6 m above the lake level, cased off with steel casing, enclosed in a suitable pump—control house.

Although option 3 guarantees the capture of groundwater flow before it reaches the lake, the problem of possible large drawdown and backflow of lake water, along with the energy required for pumping, oriented further study toward solution 1.

Following the request to avoid a mixture of ground and surface waters, the concrete elliptical structure—coffer dam has been designed and constructed. It covers a surface of some 300 m^2. Considering the importance and influence of lake water fluctuations on the intake, the special removable spillway section (rubber gate) has been designed and installed on the dam crest. The idea is to allow the non-captured spring water to overflow easily into the lake and to manipulate the height of the water level inside the coffer dam when the lake level rises (annual amplitude can be 5–6 m). The two automatic and remotely operated compressors are used to direct the air into a rubber tube and activate the gate when necessary (Fig. 16.50).

Fig. 16.50 Intake Bolje sestre and three stages of its construction

To date, the system is functioning without interruptions and failure. The minimal discharge of 2.3 m^3/s is far above actual demands. More importantly, the design and implementation of this excellent intake solution are between just 1 and 2 percent of the total investment in this complex water supply project. However, the question is, be proud of this fact or consider it an underestimation of intellectual property?

References

References to Section 16.1

Bruce DA (2003) Sealing of massive water inflows through karst by grouting: principles and practice. In: Back B (ed) Sinkholes and the engineering and environmental impacts of karst. ASCE Geotech. Spec. publ. no. 122

Fazeli MA (2005) Construction of grout curtain in karstic environment case study: Salman Farsi dam. In: Stevanović Z, Milanović P (eds) Water resources and environmental problems in karst, Proceedings of international conference KARST 2005. University of Belgrade, Institute of Hydrogeology, Belgrade, pp 659–666

Fazeli MA (2007) Construction of grout curtain in karstic environment case study: Salman Farsi Dam. Environ Geol 51(5):791–796

Ford D, Williams P (2007a) Karst hydrogeology and geomorphology. Willey, Chichester

Hidrotehnika (2012), Belgrade. Web site: http://www.hidrotehnika.rs/alzir/brana-ourkiss/

Milanović P (2000a) Geological engineering in karst. Monograph, Zebra Publ. Ltd, Belgrade

Milanović P, Stevanović Z, Beličević V (2007) Barrage Hammam Grouz, Saf Saf, Ourkiss. Raport d'Expertise, ANBT, Algeria

Milanović S, Stevanović Z, Jemcov I (2010) Water losses risk assessment: an example from Carpathian karst. Environ Earth Sci 60(4):817–827

Sahuquillo A (1985) Spanish experience in karst water resources, vol 161. IAHS Publication, Ankara

Stevanović Z, Milanović S, Ristić V (2010) Supportive methods for assessing effective porosity and regulating karst aquifers. Acta Carsologica 39(2):313–329

Stucky-Electrowatt Joint Venture (1996–2004) Salman Farsi Dam—Reports on the design of the grout curtain. Zürich

Therond R (1972) Recherche sur l'etancheite des lacs de barrage en pays karstique. Eyrolles, Paris

Vlahović M (2005) Surface reservoir in the karst of Nikšićko polje and problems of their maintenance. In: Stevanović Z, Milanović P (eds) Water resources and environmental problems in karst, Proceedings of international conference KARST 2005. University of Belgrade, Institute of Hydrogeology, Belgrade, pp 671–678

Zogović D (1980) Some methodological aspects of hydrogeological analysis related to dam and reservoir construction in karst. In: Proceedings of 6th yugoslav conference for hydrogeology and engineering-geology. Portorož, pp 283–291

References to Section 16.2

Abramov KS, Skirgelo BO (1968) Osušenie šahtnih ikarernih polej. Nedra, Moscow, p 255

Alliquander E (1982) Experience and ideas of development on the control of mining under karstic water hazard. In: Proceedings of the first international mine water congress (IMWA), Vol. B. Budapest, pp 7–18

Andreychuk VN (1996) Bereznikovsky Sink. Urals Branch of Russian Academy of Sciences, Perm, p 133

Bankovskaja MV, Krasavin PA (2004) Protection of underground waters against pollution at liquidation of mines in karst region of Kizel Coal Pool. In: Proceedings of the international symposium karstology-XXI century: theoretical and practical significance. Perm, pp 303–306

Bell KG (1963) Uranium in carbonate rocks. Shorter Contributions to General Geology. Geological Survey. Professional Paper 474-A, A1–A20

Bilopavlović V (1988) Utvrđivanje pravca kretanja podzemnih voda u području jame Trobukva-Studena vrela (Definition of groundwater flow direction in vicinity of Trobukva-Studena pithole; in Serbian). In: Proceedings of the VI Yugoslav symposium on bauxite research. Herceg Novi, pp 161–165

Bochenska T, Limisiewicz P, Poprawski L (1995) Long-term changes in the shallow water table in mining area: the Lubin-Glogow copper region, southwestern Poland. Hydrogeol J 3(3):41–52

Carta M, Ghiani M, Rossi G (1982) Uticaj rudarske industrije na okolinu: mere zaštite sa ciljem sprečavanja ili otklanjanja štete (Impact of mining industry on environment: protection measures—prevention and sanitation). In: Proceedings of the 11th world mining congress, Vol. B. Belgrade, pp 452–466

Dimitrijević DM (2013) Oksidacija pirita i kisele rudničke vode (Pyrite oxidation and acidic mining waters; in Serbian). University of Belgrade—Technical Faculty in Bor, p 187

Dragišić V, Stevanović Z (1984) O mogućnostima podzemnog isticanja dela karstnih izdanskih voda po obodu Timočke eruptivne oblasti (Possibility of subterranean inflow along the edge of Timok Eruptive Zone; in Serbian). In: Proceedings of the VIII Yugoslav Symposium on Hydrogeology and Engineering-Geology, Vol 1. Budva, pp 95–101

Dragišić V (1992) Hidrogeologija ležišta bakra istočne Srbije (Hydrogeology of copper deposits of eastern Serbia; in Serbian). University of Belgrade—Faculty of Mining and Geology, Belgrade

Dragišić V (1994) Hidrohemijske karakteristike ležišta bakra “Veliki Krivelj” (Hydrochemical characteristics of copper mine “Veliki Krivelj”; in Serbian). In: Proceedings of the XXVI October conference of miners and metallurgists. Donji Milanovac, pp 42–45

Dublyanskiy VN, Nazarova VU (2004) Karst rocks as mineral resources. In: Proceedings of the international symposium karstology-XXI century: theoretical and practical significance. Perm, pp 279–284

Ershov VV, Eremin VU, Popova BG, Tihomirov ME (1989) Geologija i razvedka mestoroždenij poleznih iskopaemih (Geology and exploration of mineral resource deposits; in Russian). Nedra, Moscow, p 399

Ford D, Williams P (2007b) Karst hydrogeology and geomorphology. Wiley, Chichester

Gongyu L, Wanfang Z (2006) Impact of karst water on coal mining in North China. Environ Geol 49:449–457

James R (1997) Mine drainage and water resources. Bull Peak District Min Hist Soc 13(4):74–80

Johnson KS (2004) Evaporite-Karst processes, distribution, and problems in the United States. In: Proceedings of the international symposium karstology-XXI century: theoretical and practical significance. Perm, pp 14–19

Kleiman BD (1982) Mine drainage in karst. In: Proceedings of the first international mine water congress (IMWA), Vol B. Budapest, pp 501–516

Korać M, Kecojević V (1988) Rezultati analize podataka geomehaničkih ispitivanja radne sredine na primjeru ležišta „Štitovo“ (Nikšić) (Results of geomechanical analyses of working environment on example of “Štitovo” mine (Nikšić); in Serbian). In: Proceedings of the VI Yugoslav symposium on bauxite research. Herceg Novi, pp 191–206

Korotkevich GV (1970) Soljanoj karst (Salty karst; in Russian). Nedra, Moscow, p 255

Lolcama J (2005) Case studies of massive flow conduits in karst limestone. 10th multidisciplinary conference on sinkholes and the engineering and environmental impacts of karst, Proceedings sinkholes engineering and environmental impacts on karst Texas, United States, pp 57–65

Lovell HL (1983) Coal mine drainage in the United States—an overview. Water Sci Tech 15:1–25

Lottermoser B (2007) Mine wastes characterization, treatment, environmental impact, 2nd edn. Springer, New York

Luković M (1939) Novija promatranja u rudniku Vrdniku u vezi sa pojavom termalne vode u potkopima (Novelties on Vrdnik Mine in connection with thermal water occurrences in the galleries; in Serbian). Compte rendu des société Serbe de géologie 1938, Belgrade, pp 13–16

Lunev BS, Naumova BO, Naumov VA (2004) Karst mineral resources. In: Proceedings of the international symposium karstology-XXI century: theoretical and practical significance. Perm, pp 23–29

Maksimovich GN (2004) Ways of the decision of environmental problems connected with development of the karst in coal-mining areas. In: Proceedings of the international symposium karstology-XXI century: theoretical and practical significance. Perm, pp 306–311

McKee DM, Hannon PJ (1985) The hydrogeological environment at the Gays River mine. Int J Mine Water 4:13–34

Miladinović B, Dragišić V (1998) Prognoza rudničkih voda u rudarskim radovima nekih ležišta uglja Senjsko-resavskog basena (Forecasting water inflow in mine works of some Senj-Resava coal basin; in Serbian), vol 8. Podzemni radovi (Ground Works) University of Belgrade—Faculty of Mining and Geology, Belgrade, pp 53–60

Miladinović B (2000) Hydrogeology of REMBAS. Zadužbina Andrejević p 110

Milanović P (2000b) Geological engineering in karst. Zebra Publishing Ltd., Belgrade

Motyka J, Czop M (2010) Influence of karst phenomena on water inflow to Zn-Pb mines in the Olkusz District (S Poland). In: Andreo B et al (eds) Advances in research in karst media. Springer, Berlin, Heidelberg, pp 449–454

Mramor J (1984) Problematika odvodnjavanja triade v rudniku lignita Velenje (Problems in dewatering of Velenje mine field; in Slovenian). In: Proceedings of the VIII Yugoslav symposium on hydrogeology and engineering-geology, Vol 1. Budva, pp 417–425

Nikolić P, Dimitrijević D (1990) Coal of Yugoslavia. Pronalazaštvo, Belgrade, p 462

Plotnikov NI, Roginec II (1987) Gidrogeologija rudnih mestoroždenij. Nedra, Moscow, p 1987

Plotnikov NI (1989) Tehnogennie izmenenia gidrogeologičeskih uslovij (Technogenetic modifications of hydrogeological conditions; in Russian). Nedra, Moscow, p 268

Radulović M, Popović Z, Damjanović M (1987) Osvrt na hidrogeološke uslove ovodnjenosti ugljonosnog basena Maoče kod Pljevalja (On hydrogeological conditions of watering of coal basin Maoče near Pljevlja; in Serbian). In: Proceedings of the IX Yugoslav symposium on hydrogeology and engineering geology, Vol 1. Priština, pp 277–288

Radulović M (2000a) Karst hydrogeology of Montenegro, vol XVIII. The Institute for Geological Explorations of Montenegro. Separate Issues of Geological Bulletin, Podgorica, p 271

Slišković I (1984) Geološko-hidrogeološke karakteristike ležišta boksitne rude Trobukva-Studena vrela i mogućnost smanjenja dotoka vode u jamske prostorije (Geology and hydrogeology of the bauxite deposits Trobukva-Studena vrela and opportunities to reduce inflows into mine pit; in Croatian). In: Proceedings of the VIII Yugoslav symposium on hydrogeology and engineering geology, Vol 1. Budva, pp 559–571

Stevanović Z, Dragišić V, Filipović B (1991) The influence of the karst aquifer on ore deposits in east Serbia, Yugoslavia. Int J Mine Water 1:114–119

Stevanović Z, Dragišić V (1995) Some cases of accidental karst water pollution in the Serbian Carpathians. Theor Appl Karstology 8:137–144

Šarin A, Tomašič M (1991) Hydrogeological review of the Raša Coal Mine in the coastal karst of Croatia. In: Proceedings of the 4th congress Intern. mine water association, Vol. 1. Ljubljana (Slovenia)-Pörtscach (Austria), pp 125–131

Tilmat G (1973) Hydrologie des gisements karstiques Francais. In: Yugoslav II (ed) Symposium on resource and exploration of Bauxites, vol A-XVII. Tuzla, pp 1–22

Tóth B (1982) Shaft drilling activity for the water protection of bauxite mines in Nyrád. In: Proceedings of the 1st congress of the Intern. mine water association (IMWA). B, Budapest, pp 244–258

Vasiljević S, Koprivica V, Nikolić R, Raonić M, Todorović M, Kilibarda S (1988) Tehnologija podzemne eksploatacije u složenim rudarsko-geološkim uslovima rudnika boksita "Nikšić" sa osvrtom na mogućnost poboljšanja i tendencije razvoja (Technology of underground exploitation in complex mining-geological conditions of Nikšić Mine—development tendencies and improvement; in Serbian). In: Proceedings of the VI Yugoslav symposium on bauxite research, Herceg Novi, pp 305–316

Wenyong P, Zhizhong L, Hongze G (1991) Ordovician limestone water control in north China coalfield, 4th Intern. mine water association congress, Ljubljana (Slovenia) – Portschach (Austria), pp 207–211

References to Section 16.3

Angel JC, Nelson DO, Panno SV (2004) A comparison of manual and GIS-based methods for determining sinkhole distribution and density: an example from Illinois' sinkhole plain. J Cave Karst Stud 66(1):9–17

Gondwe BRN, Ottowitz D, Supper R, Motschka K, Merediz-Alonso G, Bauer-Gottwein P (2012) Regional-scale airborne electromagnetic surveying of the Yucatan karst aquifer (Mexico): geological and hydrogeological interpretation. Hydrogeol J 20:1407–1425

Gregory AS, Hugh HM, Jason ED (2001) A simple map index of karstification and its relationship to sinkhole and cave distribution in Tennessee. J Cave Karst Stud 63(2):67–75

Pavlović R, Čupković T, Marković M (2001) Daljinska detekcija (Remote sensing; in Serbian). Faculty of Mining and Geology, University of Belgrade, Belgrade

Radulović M (2010) Groundwaters of Montenegro (in Serbian). In: Djordjević B, Sekulić G, Radulović M, Šaranović M, Jaćimović M (eds) Water potentials of Montenegro (in Serbian). Montenegrin academy of sciences and arts, Podgorica, pp 62–105

Radulović MM, Stevanović Z, Radulović M (2012) A new approach in assessing recharge of highly karstified terrains–Montenegro case studies. Environ Earth Sci 65(8):2221–2230

Smith BD, Smith DV, Paine JG, Abraham JD (2005) Airborne and ground electrical surveys of the Edwards and Trinity aquifers, Medina, Uvalde, and Bexar Counties, Texas. In: US Geological Survey Karst interest group proceedings, USGS, Rapid City, 12–15 Sept 2005

Supper R, Motschka K, Ahl A, Bauer-Gottwein P, Gondwe B, Alonso GM, Romer A, Ottowitz D, Kinzelbach W (2009) Spatial mapping of submerged cave systems by means of airborne electromagnetics: an emerging technology to support protection of endangered karst aquifers. Near Surf Geophys 7(5–6):613–627

Won-In K, Charusiri P (2003) Enhancement of thematic mapper satellite images for geological mapping of the Cho Dien area, Northern Vietnam. Int J Appl Earth Obs Geoinf 4(3):183–193

Wynnea JJ, Timothy NT, Diazd GC (2008) On developing thermal cave detection techniques for Earth, the Moon and Mars. Earth Planet Sci Lett 272(1–2):240–250

Zurbuchen L, Kellenberger T (2008) Detection of cave entrances with airborne thermal imaging. EGU General Assembly, University of Zurich, Vienna, pp 13–18

References to Section 16.4

Al Charideh AR (2007) Environmental isotopic and hydrochemical study of water in the karst aquifer and submarine springs of the Syrian coast. Hydrogeol J 15:351–364

Alfirević S (1963) Hydrogeological investigations of submarine springs in the Adriatic. AIH Publ. Réunion de Belgrade. Comité National Yougoslave pour la Géologie de Génie Civil et l'Hydrogéologie, Belgrade, pp 255–264

Arandjelović D (1976) Geofizika na karstu (Geophysics in karst). Spec. ed, Geozavod, Belgrade

Arfib B, Dörfliger N, Wittwer C (2005) General overview of seawater intrusion in coastal aquifers. In: Cost Environment Action COST 621, Tulipano L, Fidelibus MD, Panagopoulos A (eds) Groundwater management of coastal karstic aquifer. COST Office, Luxemburg, pp 76–80

Back W (1992) Coastal karst formed by ground-water discharge. Yucatan, Mexico. In: Paloc H, Back W (eds) Hydrogeology of selected karst regions. International contributions to hydrogeology, IAH, vol 13. Heise, Hannover, pp 461–466

Bakalowicz M, Fleury P, Dörfliger N, Seidel JL (2003a) Coastal karst aquifers in Mediterranean regions. A valuable ground water resource in complex aquifers. vol 2, no 8. IGME Publ., Technologia de la Intrusion de Agua de Mar en Acuiferos Costeros: Paises Mediterraneos (TIAC). Hydrogeologia y aguas subterraneas, Alicante, pp 125–140

Bakalowicz M, Fleury P, Jouvencel B, Prome JJ, Becker P, Carlin T, Dörfliger N, Seidel JL, Sergent P (2003b). Coastal karst aquifers in Mediterranean regions. A methodology for exploring, exploiting and monitoring submarine springs. Technologia de la Intrusion de Agua de Mar en Acuiferos Costeros: Paises Mediterraneos, IGME, Madrid, pp 673–680

Biondić B, Goatti V (1984) La galerie souterraine "Zvir II" a Rijeka (Yougoslavie). In: Burger A, Dubertret L (eds) Hydrogeology of karstic terrains. Case histories. International contributions to hydrogeology, IAH, vol 1, Verlag Heinz Heise, Hannover, pp 150–151

Biondić B, Biondić R (2003) State of seawater intrusion of the Croatian coast vol 2. IGME Publ., TIAC, Tecnologia de la Intrusion de Agua de Mar un Acuiferos Costeros: Paises Mediterraneos, Alicante, pp 225–238

Bonacci O (1987) Karst hydrology with special reference to the Dinaric karst. Springer, Berlin

Burger A, Dubertret L (eds) (1984) Hydrogeology of karstic terrains. Case histories. International contributions to hydrogeology, IAH, vol 1. Verlag Heinz Heise, Hannover

Cost Environment Action COST 621 (2005) Tulipano L, Fidelibus MD, Panagopoulos A (eds) Groundwater management of coastal karstic aquifer. COST Office, Luxemburg

Dörfliger N, Fleury P, Bakalowicz M, El-Hajj H, Al Charideh A, Ekmekci M (2010) Specificities of coastal karst aquifers with the hydrogeological characterisation of submarine springs—overview of various examples in the Mediterranean basin. In: Bonacci O (ed) Sustainability of the karst environment—Dinaric karst and other karst regions. IHP series on Groundwater-VII/2010/GW-2, UNESCO, Paris, pp 41–48

Drogue C and Bidaux P (1986) Simultaneous outflow of fresh water and inflow of sea in a coastal spring. Nature 322/6077:361–363

Drogue C (1996) Groundwater discharge and freshwater-saline water exchange in karstic coastal zones. In: Proceedings of international symposium groundwater discharge in the coastal zone, vol 8. LOICZ-IGBP, LOICZ reports and studies, Moscow, pp 37–43

Eftimi R (2003) Some considerations on seawater-freshwater relationship in Albanian coastal area vol 2. In: IGME Publ., TIAC, Tecnologia de la Intrusion de Agua de mar un acuiferos Costeros: paises mediterraneos, Alicante, pp 239–250

Fleury P, Bakalowicz M, de Marsily G (2007) Submarine springs and coastal karst aquifers: a review. Hydrol J 339:79–92

Komatina M (1984) Control of underground flow in the littoral karst, Orebic, Yugoslavia. In: Burger A, Dubertret L (eds) Hydrogeology of karstic terrains. Case histories. International contributions to hydrogeology, IAH, vol 1. Verlag Heinz Heise, Hannover, pp 156–159

Lapierre L, Creuse V, Jouvencel B (2008) Robust diving control of an AUV. Ocean Eng 36(1):92–104

Mijatović B (1983) Problems of sea water intrusion into aquifers of the coastal Dinaric karst. In: Mijatovic B (ed) Hydrogeology of the Dinaric Karst, Field trip to the Dinaric karst, Yugoslavia. “Geozavod” and SITRGMJ, Belgrade, pp 89–108 15–28 May 1983

Mijatović B (1984) Captage par galerie dans un aquifere karstique de la cote Dalmate: Rimski bunar, Trogir (Yougoslavie). In: Burger A, Dubertret L (eds) Hydrogeology of karstic terrains. Case histories. International contributions to hydrogeology, IAH, vol 1. Verlag Heinz Heise, Hannover, pp 152–155

Mijatović B (2007) The groundwater discharge in the Mediterranean karst coastal zones and freshwater tapping: set problems and adopted solutions. Case studies. Environ Geol 51:737–742

Milanović P (2000c) Geological engineering in karst. Dams, reservoirs, grouting, groundwater protection, water tapping, tunnelling. Zebra Publishing Ltd, Belgrade, p 347

Potié L, Ricour J, Tardieu B (2005) Port-Miou and Bestouan freshwater submarine springs (Cassis—France) investigations and works (1964–1978). In: Stevanović Z, Milanović P. Water resources and environmental problems in Karst. Proceedings of the international conference KARST 2005, University of Belgrade, Institute of Hydrogeology, Belgrade, pp 249–257

Radulović M (2000b) Karst hydrogeology of Montenegro. Special issue of geological bulletin, vol. XVIII. Spec. Ed. Geol. Survey of Montenegro, Podgorica, p 271

Stevanović Z (2010a) Major springs of southeastern Europe and their utilization. In: Kresic N, Stevanović Z (eds) Groundwater hydrology of springs. Engineering, theory, management and sustainability. Elsevier Inc. BH, Amsterdam, pp 389–410

Stevanović Z (2010b) Intake of the Bolje Sestre karst spring for the regional water supply of the Montenegro. In: Kresic N, Stevanović Z (eds) Groundwater hydrology of springs. Engineering, theory, management and sustainability. Elsevier Inc. BH, Amsterdam, pp 457–478

Stevanović Z, Eftimi R (2010) Karstic sources of water supply for large consumers in southeastern Europe—sustainability, disputes and advantages. Geol Croat 63(2):179–186

Stringfield VT, LeGrand HE (1971) Effects of karst features on circulation of water in carbonate rocks in coastal areas. Hydrol J. 14:139–157

Zektzer IS, Ivanov VA, Meskheteli AV (1973) The problem of direct groundwater discharge to the seas. Hydrol J 20:1–36